LGURJCSIT Volume 06, Issue 02, Article ID 272, 26 pages
https://doi.org/10.54692/lgurjcsit.2022.0602272

MM-Wave HetNet in 5G and beyond Cellular Networks Reinforcement Learning Method to improve QoS and Exploiting Path Loss Model

Asad Ali[a], Muhammad Khawar Bashir [b], Amir Ali [b], Muhammad Waseem Razzaq [c]

[a] Department of Electrical Engineering, Superior University, Lahore
[b] Department of Statistics and Computer Science, University of Veterinary & Animal Sciences, Lahore
[c] Department of Electrical Technology, Government College of Technology, Sahiwal

Received 27 May 2022; Accepted 25 June 2022; Published 28 June 2022

Abstract:

This paper presents High density heterogeneous networks (HetNet) which are the most promising technology for the fifth generation (5G) cellular network. Since 5G will be available for a long time, previous generation networking systems will need customization and updates. We examine the merits and drawbacks of legacy and Q-Learning (QL)-based adaptive resource allocation systems. Furthermore, various comparisons between methods and schemes are made for the purpose of evaluating the solutions for future generation. Microwave macro cells are used to enable extra high capacity such as Long-Term Evolution (LTE), eNodeB (eNB), and Multimedia Communications Wireless technology (MC), in which they are most likely to be deployed. This paper also presents four scenarios for 5G mm-Wave implementation, including proposed system architectures. The WL algorithm allocates optimal power to the small cell base station (SBS) to satisfy the minimum necessary capacity of macro cell user equipment (MUEs) and small cell user equipment (SCUEs) in order to provide quality of service (QoS) (SUEs). The challenges with dense HetNet and the massive backhaul traffic they generate are discussed in this study. Finally, a core HetNet design based on clusters is aimed at reducing backhaul traffic. According to our findings, MM-wave HetNet and MEC can be useful in a wide range of applications, including ultra-high data rate and low latency communications in 5G and beyond. We also used the channel model simulator to examine the directional power delay profile with received signal power, path loss, and path loss exponent (PLE) for both LOS and NLOS using uniform linear array (ULA) 2X2 and 64x16 antenna configurations at 38 GHz and 73 GHz mmWave bands for both LOS and NLOS (NYUSIM). The simulation results show the performance of several path loss models in the mmWave and sub-6 GHz bands. The path loss in the close-in (CI) model at mmWave bands is higher than that of open space and two ray path loss models because it considers all shadowing and reflection effects between transmitter and receiver. We also compared the suggested method to existing models like Amiri, Su, Alsobhi, Iqbal, and greedy (non adaptive), and found that it not only enhanced MUE and SUE minimum capacities and reduced BT complexity, but it also established a new minimum QoS threshold. We also talked about 6G researches in the future. When compared to utilizing the dual slope route loss model alone in a hybrid heterogeneous network, our simulation findings show that decoupling is more visible when employing the dual slope path loss model, which enhances system performance in terms of coverage and data rate.

Keywords: Millimeter-Wave (MM-Wave), Heterogeneous Networks (HetNet), 5G to 6G Challenges, scenarios and Gaps, Future Forecast of 5G to 6G, Path Loss Models, QoS using WL model

I. Introduction

High-performance devices, such as mobile tablets, smart-watches, and smart-phones, are fast increasing in number. To overcome the limits of existing cellular devices, the fifth generation (5G) cellular network was launched. The demand for data intensive mobile applications is growing exponentially [1].

A cellular network is a network that connects a base station (BS) to a base station controller (BSC), and subsequently to a mobile core network, and it has made significant progress in new technology, services, and applications. Significant advances in wireless technology and standardization have enabled cellular networks to provide faster data rates, greater coverage, more applications, more connected devices, and strict quality of service (QoS). High-speed

packet communications, the long-term development of HSPA (LTE), improved LTE and Wi-Fi, and different cell sizes with dense cell distribution and different physical locations sponsored by different solution providers (i.e. media providers). It can realize the multiplexing of the spatial spectrum and improve the spectrum performance [2].

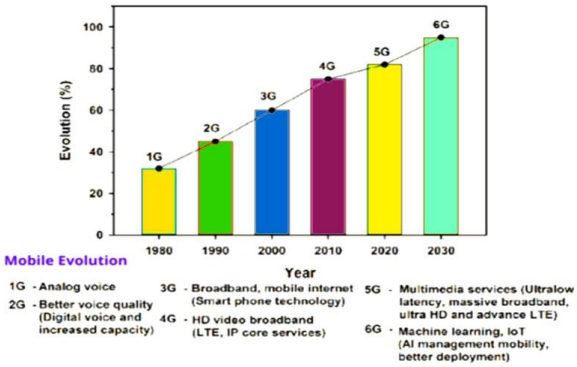

Fig.1. Evolution of Mobile Technologies from 1G to 6G [11].

As cellular networks become denser and more heterogeneous by including small cells such as pico-cells and femto-cells, self-organization becomes more and more important. In Fig. 1, evolution of Mobile technologies is shown as there is no doubt that no technology can meet the strict 5G specifications. These specifications include increased bandwidth and better quality of Experience (QoE) while supporting multiple wireless connections for human-machine and computer applications, both of which have different characteristics. The emergence of HetNet represents a major change in today's network architecture, indicating that the central macro-cell system can evolve into a more autonomous combination. Reinforcement learning (RL) is one of the methods to alleviate interference in HetNet, and it provides many advantages for solving the best solution problem in integrated methods. In this article, we introduced our vision for 6G wireless deployment solutions, performance indicators, and future cutting-edge technologies [3]. With the beginning of next-generation networks, the use of second-generation (2G) services is decreasing. 3G networks are introduced every day. Global coverage, all spectrums, complete implementation, and strong or inherent defenses are the latest paradigm shifts. The 6G radio network has expanded from ground 1G-5G networks to interconnected air-air-land-sea networks, including satellites, unmanned aerial vehicles (UAV), ultra-dense ground networks (UDN), underground communications, maritime communications, and submarine communications. The expansion of 5G networks is expected to begin in 2021. In the next five years, there are plans to exceed 1 billion 5G users, accounting for 12% of all cellular users. The result is a video application that requires high bandwidth, consistent coverage, and performance [4]. There are higher requirements for flow. The wireless 5G data network will be available worldwide starting in 2021. On the other hand, from 2030, 5G cannot meet all the standards of future networks. A self-organizing network (SON) can be self-optimized, optimized, and repaired. The basic tasks include the establishment of a new base station (BS), resource management, and network fault management. As a result, from two perspectives, the future wireless network will maintain an extremely heterogeneous state to meet the efficiency requirements of 5G: In order to be able to exchange massive amounts of data at different frequencies, secure and almost instant broadband is required, which must be supported by 6G wireless network. Smart devices in the Internet of Things are a solution because they can provide extremely reliable, powerful, efficient, and stable communications. Due to a large amount of available bandwidth in the 60 GHz band that can support extremely high data rates (i.e., up to 6.7 Gbps), 60 GHz wireless networks have recently received widespread attention [5]. This is also called mm-Wave, and it paved the way for the introduction of Gigabit Wi-Fi. The wireless upgrade from 1G to 4G is a significant step forward in the expansion of internet and cellular data. 5G has evolved from 4G mobile broadband (MBB) to (eMBB) and the Internet of Things in terms of hardware standards. For future 6G wireless communication systems, such a modulation method will provide low-complexity architecture with low latency and great data transmission spectrum efficiency. Through clean data exchange, data exchange in 6G can exchange information, knowledge, and experience as well as historical data, current attributes, and future possibilities. Such a modulation scheme will provide low-complexity architecture for future 6G wireless communication systems, with low latency and high data transmission spectrum efficiency. A dense HetNet environment, on the other hand, has its own collection of issues, including intrusion, spectrum management, and energy management. Small cells, which are an integral part of HetNet, will be critical to the efficient deployment and realization of the 5G environment, and HetNet will become a central network in the 5G environment [6]. The use of the millimeter (mm-Wave) frequency spectrum is certain

for basic methods of delivering planned high-speed communications between 5G cellular networks.

TABLE 1 COMPARISON with 3G to 6G Generations [46].

Technology / features	**3G**	**4G**	**5G/6G**
Data Bandwidth	2Mbps	2Mbps to 1Gbps	1Gbps & Higher (as demand)
Frequency Band	1.8 - 2.5 GHz	2 - 8 GHz	3-300GHz
Standards	WCDMA CDMA-200 TD-SCDMA	All access convergence including: OFMDA, MC-CDMA Network-LMPS	CDMA & BDMA
Technology	Broad bandwidth CDMA,IP technology	Unified IP, seamless combination of broadband LAN/WAN/ PAN and WLAN	Unified IP and seamless combination of broadband, LAN/WAN/PAN/ WLAN and technologies for 5G new deployment (could be OFDM etc.)
Service	Integrated high quality audio, video and data	Dynamic information access, wear-able devices, HD streaming, global roaming	Dynamic information access, wear-able devices, HD streaming, any demand of users; upcoming all technologies, global roaming smoothly
Multiple Access	CDMA	CDMA	CDMA & BDMA
Core Network	Packet Network	All IP Network	Flatter IP Network & 5G Network Interfacing(5G-NI)
Definition	Digital Broadband, packet data	Digital Broad band, Packet data, All IP	Digital Broadband, Packet data All IP, Very high Throughput
Hand off	Horizontal	Horizontal & Vertical	Horizontal & Vertical

Table 1, depicts the generational contrasts so far [15], [46]. A group of researchers invented a new method to solve heterogeneous networks, which solved the following situation: MM-Wave communication based on mm-Wave base station (BS) coverage in macro cell (HetNet) is used [7]. Coverage area of small cells is often comparable to the coverage area of a field. The effect of inter-site range on overall output transfer to Long Term Evolution-Advanced (LTE-A) HetNet was investigated by [8], which is the most recent work up to expectation on the fundamental importance of this work in this paper.

Cells in the fifth-generation (5G) cellular system must increase system capacity or provide absolutely low latency, reliability, and network protection [9] and [10] in order to manage large amounts of data (things) across the mobile consumer (US) Internet of Things (Iot) and networking equipment. For advanced regulatory multiplexing, the use of heterogeneous base stations (such as picocells, femtocells, transmission, and circular wireless cables) has been concentrated on a large scale. Fig. 2 depicts the structures of mm-wave cells running in the 50-400 GHz band [12]. Users of 4G networks connect to networks that operate at a frequency of 50 MHz. Nonetheless, all directional searches will necessitate mm-Wave interactions, which will increase the signaling overhead [13]. Furthermore, after removing all search ambiguity, some works from the literature were introduced to decrease the high signaling overhead that comes with it [14]. By accessing mm-Wave Structured Cabling System (SCs) within the user plane, the power plane (C-plane) provides constant and coherent legacy Long term evolution (LTE) coverage, while the User equipment (UE) receives higher data rates (U-plane). Furthermore, due to strong signaling, this paper introduces a cluster-oriented average HetNet architecture to reduce backhaul traffic in 5G HetNet based on mm-Wave [15]. The remainder of the paper is organized as follows: In Section 2, the future technology of 6G is well described, and the system model of 5G and 6G

are presented. In section 3, wireless 5G network requirements, research challenges, and gaps for the mm-wave HetNet are presented. Radio resource management with different approaches is presented as well. A case study requirement for mm-wave HetNet is also presented. Section 4 contains the learning frame network of mm-wave HetNet for solving the optimization problem is presented and proposed the WL Based algorithm in HetNet for the power allocation of the system. A comparison is made with recent models such as; Amiri, Su, Alsobhi, Iqbal and greedy (non adaptive) and WL algorithms in Simulation setup of different scenarios as well as the future extension work and conclusions are presented.

II. Related Work:

Millimeter-wave frequencies vary from 30 to 300 GHz, whereas terahertz frequencies range from 0.1 to 10 THz. As a result, the 100-300 GHz frequency band exhibits various millimeter wave and terahertz wave properties, including wide bandwidth, strong directivity, noticeable path loss, blocking effects, atmospheric absorption, and increased scattering. Small cell communication networks mostly use large-area millimeter waves (mm-Wave) (very high frequencies in the range of 30 to 300 GHz). The RF mm-Wave backhaul network also uses the 6 GHz to 60 GHz range. As a result, the shorter wavelengths in its spectrum make the integration of multiple antennas and small cells easier, enabling massive MIMO in applications other than LOS. Despite the fact that millimeter waves may deliver data rates of several hundred meters per second over various gigahertz bandwidths, terahertz frequencies can attain data rates of one billion megabytes per second across various tens of gigahertz bandwidths. As a cellular solution for small cellular networks, millimeter-wave networks are an emerging trend in 5G mobile systems. However, in this case, the antenna array and RF components (beamforming and modulation scheme) of the transceiver are critical to the research. In the terahertz range, atmospheric absorption and diffuse scattering are more extreme than in the millimeter-wave wavelength range. However, in the industrial IoT environment, millimeter-wave channel measurement is also expected to achieve potential batch connections at high data rates. A portion of the proposed mm-Wave clustered HetNet architecture is presented in this section. The current relationship model is also updated and extended by the mm-Wave.

A. Architecture for 5G Mm-Wave-based HetNet

Fig. 3 depicts the proposed 5G HetNet architecture based on mm-Wave [19]. As shown in Fig. 3, the Long term evolution (LTE) Mobile Communication system (MC's) massive coverage is superimposed on several mm-Wave Structured Cabling System (SCs) as an alternative to the legacy LTE HetNet under 6 GHz SCs [20].

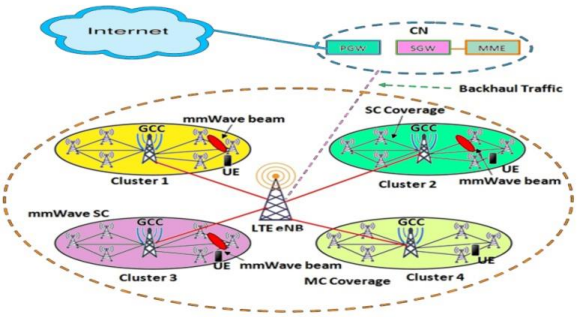

Fig.3. For 5G, a clustered of mm-Wave HetNet network architecture has been proposed.

Femtocell clustering is based on grouping interfering femtocells into a cluster, which eliminates co-tier interference while allowing for high scalability. The proposed architecture involves in Fig. 3, the presence of each GCC via the X2 interface of the E-UTRAN Node B (eNB) through the Packet Data Network (PGW), Serving Cisco Gateway (SGW), and Mobility Management Unit (MME). As the S1 interface (eNB). There are four stages of resource allocation based on femtocell grouping. When one hops away from the neighboring femtocell, all eNodeBs (eNB) is created first, and then the interference neighbor list is sent. ENB selects the most destructive cluster head in order to calculate the degree of interference in the immediate vicinity of the jump [21]. The cluster head allocates Pseudo random binary sequence (PRBs) in the next step, with the goal of minimizing the difference between the numbers of Pseudo random binary sequence (PRBs) needed and the number of PRBs allocated. The next step is to allocate the spectrum in an orthogonal manner to reduce cross-tier overlap and increase spectral performance. In the final stage, input from each Femto user equipment (FUE) is available, which is sent to its related eNBs in the case of Pseudo random binary (PRB) collisions, which occur when multiple clusters share the same Pseudo random binary sequence (PRBs).

MM-wave HetNet for 5G advantages, application and limitation are given as under.

B. Advantages

- Lay Narrower must be disagreed with by Beam. Because of the similar type of antenna, the beam diameter is decreased as the frequency is increased.
- The mm-wave's high bandwidth allows it to measure the average performance of the spectrum after having a higher transmission rate, making it more immune to interference later on. The mm-wave's high bandwidth allows it to measure the average performance of the spectrum after having a higher transmission rate, making it more immune to interference later on.
- If it is not equipped with "fully used vehicle" (V2X) technology, tracking vehicles, motorcycles and pedestrians can make tracking easier.
- Sensing statistics will remain old in conjunction with useful resources during the establishment of the mm-Wave communication connection [24] and colleagues For example, on an mm-Wave communication exchange; a Remote Service Unit (RSU) technology established radar unit could be used in conjunction with assist monitor potential recipients to reduce beam level time, according to [25] and others.
- The Remote Service Unit system (RSU's) sensing provides cities with a steady supply of sensor data. When additional sensors, such as weather and pollution sensors, are added, the benefits can be enhanced.
- The antenna frequency and size are inversely proportional to each antenna, decreasing the hardware size.

C. Limitation

- Significant waste occurs at much too frequent intervals before performance standards were hardly used for long-distance applications [26].
- As more frequencies (such as oxygen and clouds) interfere, more research is needed to reduce the amount of interference.
- Aerospace astronomy, satellite communications, high-resolution radar, security scanning, amateur radio, and other applications are the most pressing challenges.

D. 5G Wireless Network Requirements for mm-wave HetNet

The 5G remote system is no longer institutionalized at this time. The factor, as well as careful specialized details of this device, will be available soon [27]. At least one composer is required for complete assembly in order to preserve the 5G system's characteristics [28] and other colleagues.

As a result, [29] expect that peak information fees will remain high, despite the fact that the 5G device is a valuable resource for both high- and low-portability customers. The latency requirement is usually more difficult to meet than the information charge because it needs the facts to be transmitted to the vacation spot [30].

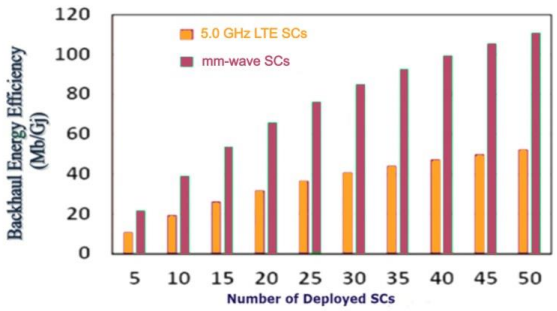

Fig.4. Backhaul network energy efficiency for various numbers of standardized cabling systems (SCs).

Furthermore, as shown in Fig. 4, the mm-Wave HetNet consumes less energy than the Long term evolution (LTE) HetNet [31], arranging is a full-size problem to solve. Transportable directors will actually smarten up the situation and plan secure system hubs Base stations (BSs), such as full-size numbers and regions, miniaturized scale, and Pico, BSs. [39]. Despite, the usefulness of this website acquisition strategy for the distant 5G HetNet must be evaluated.

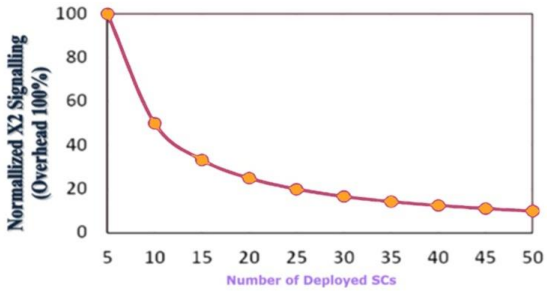

Fig.5. Normalized Backhaul overhead for X2 signaling in the traditional mm-Wave HetNet.

The quality of service (QoS) standards for 5G systems are very strict and difficult to achieve. The main advantages of QoS include uninterrupted flexibility, high efficiency, long life, high latency, extremely high data rates, long life, reduced product lines, and lower prices. The Normalized Backhaul overhead for X2 signaling in the traditional mm-Wave HetNet is shown in Fig. 5. It must be reliable and timely, and it needs to release resources effectively and access resources in a timely manner. Because people rely on their decisions, smart cities, e-medicine, and traffic management urgently need reliability with extremely low and extremely high latency [23]. To achieve a mix of low latency and high reliability, control, adaptation, coding, and modulation channel topologies are used.

E. mm-wave HetNet Research challenges, gaps

Existing developments in mobile broadband will be strengthened with designs like high-speed packet access (HSPA) and long-term development (LTE), and the advent of five technical information systems (5G) will avoid standard radio access problems with the association after 2021 [34]. Due to the fact that there are many types of computer system style correspondences, [35], In comparison to these, 5G provides completely accelerated stipulations in existing isolated networks. Although Mm-Wave's progress is still a long way from the Het Net merger, they are used to simulate that they will reflect our specific 5G network requirements. Depending on the controller, the basic problem of massive multiple-input (MIMO) is similar. , Discuss unfinished tasks and actual plans. Millimeter communication will be a fantastic help for wireless entry to connect. A dramatic illustration transition between web usage and multimedia traffic is found at the same time. As a result, the network infrastructure's and structure's characteristics will gradually change. In contrast to 4G imitations, a disparity in frequency selection necessitates an entirely limited bulk cell phone or, as a result, a significantly wide-scale roll out on cellular inferior rank websites. Outside of the front/backhauling networks, which are entirely reliant on optical string networks, the extremely small number of cell phones, followed by the extremely high choice of cell phone throughput, considerably increases the requirements. As a result of the failure of traditional alternatives such as CPRI backhauling networks, options such as analog mm-wave radio over fiber which becomes more common [36], [37]. Despite any substantial progress, a formidable challenge still stands in the way, according to the mm-wave hyperlink for 5G mobile broadband. In addition to decorating and ensuring good coverage while maintaining reliability, major improvements in regulatory design are required [38]. In order to consider the increased transmission range, a highly directional antenna or a steerable antenna beam is required. Based on space diversity, similar techniques have been used to achieve strong signal performance.

III. HetNet

Heterogeneous cellular networks [23], [34] and [35] are a new network design for cellular network operators that has dominated architectural models in the recent decade, starting with LTE release 8. (4G network). In contrast to homogeneous cellular networks (which consist of the repetitive placement of homogeneous network elements with respect to coverage area, capacity specifications, and capabilities), the HetNet architecture makes use of radio coverage elements with varying specifications and capabilities in terms of transmit power, antenna type, and functionalities (coverage capabilities, inter-communication with other elements, backhauling capabilities, and so on), resulting in a mash-up. However, in single-input single-output (SISO) and multiple-input multiple-output (MIMO) systems, finding an effective solution for joint optimization is difficult. The most basic UP technique is random pairing, in which the BS selects individuals at random to form clusters. Wireless network densification has the potential to significantly boost user throughput and network trac capacity.

IV. A LEARNING FRAMEWORK FOR SOLVING THE OPTIMIZATION PROBLEM in HetNet

Self-organizing network (SON) technology reduces the total cost of ownership of Wi-Fi networks by eliminating manual hardware configuration and dynamically optimizing performance and interruptions during maintenance. Thresholds based on QoE [50] are part of the future performance standards of LTE and 3GPP cellular networks. SON technology is also used in cellular network operators, backhaul and radio access fields as mentioned in Fig. 6.

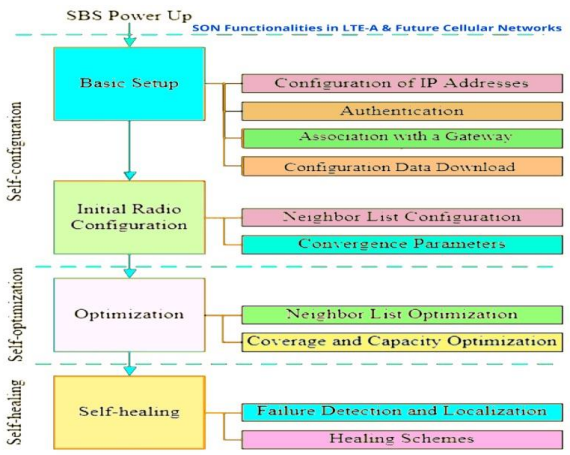

Fig.6. Long-Term Evolution-advanced (LTE-A) and Future Cellular Networks SON Functionalities.

The power consumption of the base station does not only depend on the user load. Even without users, various functions require energy. SON research and related mobile optimization ecosystems: 2015–2021" include key market dynamics, challenges, savings opportunities, use cases, SON case studies, future roadmaps, value chain analysis, and strategies. The report studies the Son ecosystem and related ecosystems to optimize cellular networks. [51]. They collect information about their environment in order to apply it and learn from it [52]. An environment and an agent make up a Reinforcement Learning (RL) scheme, and both take steps to make communication with the environment based on policies. The environment receives input after each iteration, which is used to update the environment's status [1], [53].

V. PROPOSED WL BASED ALGORITHM IN HetNet for POWER ALLOCATION

The following equation is sequentially modified to solve $W_p(y,c)$ at time t. The SC HetNet network is used as a multi-agent MDP, and then a WL-based algorithm is proposed as;

$$W^{t+11}(y_t,c_t) = (1-\alpha)W^t(y_t,c_t) + \alpha\left\{E_{t+1} + \underbrace{\gamma \underbrace{max}_{c'} W^t(y_{t+1},c')}_{E_f}\right\} \quad (1)$$

The discount factor γ is used to describe the cost function. E_f is the estimated value of the total return that may be obtained currently. In the current state, the reward amount is E_{t+1}. For example α is the learning rate that helps prevent premature convergence of the algorithm;

$$H_y^t = max_{d\in C} W^t(y,d) \quad (2)$$

The WT is shown in Table 3 as a 3D table, which contains columns and rows with status and behavior. Use the W table (WT) above to calculate the W function (WF) [1].

Algorithm 1: W-Learning Algorithm

Define states Y_t *and action* C_t

Initialize W-Table arbitrarily i.e. $W(y_t,c_t)$ *at* $t = 0$

For Iterations $\leq N_{itrations}$ ***do***

  Initialize state y_t *as* y_0

  For Step $\leq N_{step}$ ***do***

    Select y_t from C

    Apply $y_t \leftarrow EEP\ (y_t, W^t, Y, C)$

    Observe E_t

    New State y_{t+1}

    Update W-Table $W^{t+1}(y_t,c_t) =$

    $(1-\alpha)W^t(y_t,c_t) + \{E_{t+1} + \gamma H^t(y+1)\}$

    Set $y_t \leftarrow y_{t+1}$

  End

End

Table 3
The W-Table (WT) is a table that is centered on states in the rows and behavior in the columns [1].

States	Actions			
	$C_1 = P_{min}$			$C_{N_{power}} = P_{max}$
$X_1 = (0,0)$	$W(X_1,c_1)$	$W(X_1,c_2)$	...	$W(X_1,C_{N_{power}})$
$X_2 = (0,1)$	$W(X_2,c_2)$	$W(X_2,c_2)$	...	$W(X_2,C_{N_{power}})$
.				.
.			...	.
.				.
$X_n = (N_1,N_2)$	$W(X_n,c_1)$	$W(X_n,c_2)$	...	$W(X_n,C_{N_{power}})$

After changing all entries in table W, the following table will be used to calculate the best working value for each condition;

$$c = \arg\max_{d \in C} w^t(y, d) \quad (3)$$

The WL algorithm used in this analysis is described in Algorithm 1. At each time point t, the operation will be selected according to the granularity or granularity strategy function mentioned below.

$$c_t = \begin{Bmatrix} \arg\max_{c \in C} W^t(y, d) & exploitation \\ rand_{c \in C} & exploration \end{Bmatrix} \quad (4)$$

The odds for exploitation and discovery are $1 - \varepsilon$ and respectively. The self-interested" policy exploitation $\varepsilon -$ is used in Eq. (4) to apply exploitation and exploration [1].

A. MM-Wave HetNet in Wireless Communications

With the new popularity of mm-Wave characteristics in cell phone systems, this segment starts to grow, revealing problems as well as very rules [1]. Professor Akhtar in [2] believes that if the open space and his colleagues comply with the 38, 48, 70, and 83 GHz propagation power regulations, millimeter waves will help celebrate his work at the University of New York (York University) University of Texas at Austin). A health professor explained that the beamforming and multiple inputs multiple outputs (MU-MIMO) between the millimeter-wave group and the staff are due to the improvement of the charging performance of the smart-phone body [44].

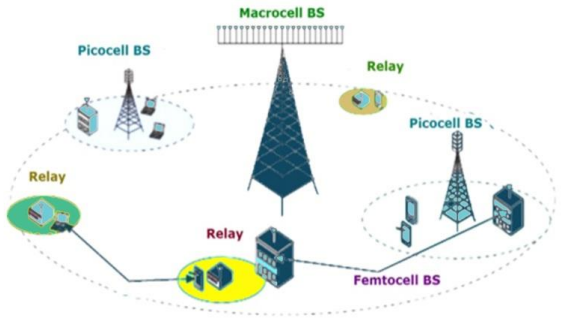

Fig.7. Femtocells and a HetNet with a macrocell BS, as well as multiple supporting Relays and picocell BSs

After assembly, the widely accepted notion of heterogeneous networks (HetNet) shows in Fig. 7. These networks can better match the needs of customers and improve standard mobile network throughput by [45] using smaller and more sophisticated cells, according to [25], [12], as is one over the latest 5G institutionalization of benchmark body engineering despite the fact that mm-Wave developments at 28 GHz have been used for rapid 5G affiliation in South Korea, the United States, and Japan, there is a need for more in-depth discussions about the circumstances, using conditions that are then applicable in accordance with empowering technologies in that area. Despite its many benefits, the mm-wave interface for 5G flexible broadband has been portrayed in a negative light to this point. Significant changes to formal material are required to enhance or guarantee outstanding inclusion, then association consistency [46]. The following are the parameters that are affected by mm-wave HetNet:

B. Bandwidth of MM-waves

Can do full duplex in a group setting at speeds approaching public Gbps [47].

Table 4
Requirements for quality of service (QoS) in 5G RIM and EEM schemes [2].

Schemes	Number of Massive devices	Huge Traffic	Use of Diverse Cases
Power control in multi-tier	✔	✔	✔
CoMP based transmission	✘	✔	✔
AIM based	✔	✔	✘
MIMO channels-based	✔	✔	✔
Cross layer based	✔	✔	✔
DPS	✔	✔	✔
Energy harvest based	✔	✔	✔
Indoor communication based	✔	✔	✘
Cooperative	✔	✔	✘

C. Mm-wave Interference Resistance Beam Width

Cross signal cure is an essential limiting issue for the purpose, particularly for Ring, Hub, and fowl typologies that use low-frequency signals. In Table 4

RIM and EEM schemes in 5G with quality of service (QoS) requirement are shown [2]. As a result, the attractive or nice area unit of mm-waves corresponds to its narrow-focused beams [48], [49]. The ability to set up 5 G technology now provides and upgrades wonderful features such as bidirectional limited transmission capacity, extreme file speeds, unrealistic requirements, and super Quality of Service (QOS).

VI. DESIGN METHODOLOGY

In mm-Wave, we assume that each unit uses the entire spectrum. Due to the high attenuation in each frequency range, the coverage of the millimeter-wave unit is particularly limited. As a result, there is no harmful interference when reusing the entire spectrum. As a result, we assume that each millimeter-wave BS uses the full spectrum. In this case, it is meaningless to consider RB granularity, especially when flexibility is reduced. Combined with mm-Wave BS $j \in J^{mmW}$, the SINR observed by user $i \in I$ can be expressed as;

$$SINR_{ij}^{mmw} = \frac{p_j g_j g_i \gamma_{ij}}{\sum j' \epsilon J_{j' \neq j}^{mmw} p_{j'} g_{j'} g_i \gamma_{ij'} + P^{\sim} N} \quad (5)$$

BS mm-Wave and LTE use different carrier frequencies, antenna heights, and different types of environments, so the degree of attenuation is different. As shown in Fig. 6, we concentrate on the multi-tiered ultra-dense HetNet scenario, in which quite a lot of Structured Cabling System (SCs) is deployed under the overlaid Media Converter Fiber (MC). Regardless of whether the Structured Cabling (SC) cluster is close to the Macro cell base stations (MBS) or at the cell edge, MBS interference badly degrades Specialized User Equipment & System (SUE), Quality of service (QoS). The red-dotted arrows in Fig. 7 reflect this intrusion, which is cross-tier [16].

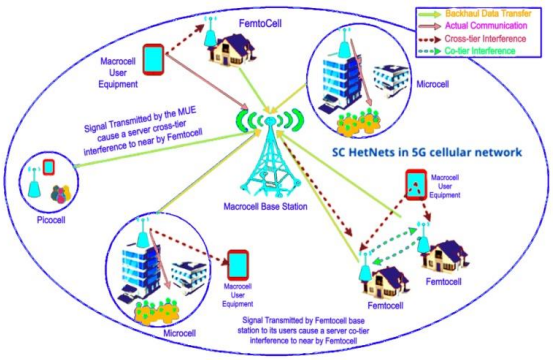

Fig.8. In 5G cellular networks, the HetNet structured cabling system (SC) model covers the disputes between layers.

Although Small Cell Basic Stations (SBS) transmission ability is decrease than Macro Cell Basic Stations (MBS), Maco User Systems (MUE) close to SBS are prone to interference with SBS in Fig. 8, thereby decreasing the excellent of the MUE service (QoS) [17].

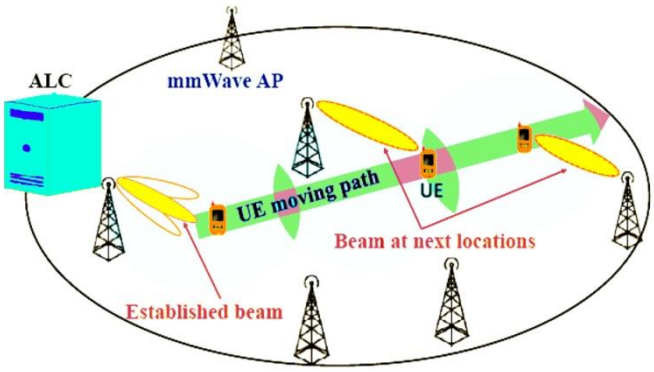

Fig.9. System architecture Model of mm-wave.

A model of the millimeter-wave architecture is demonstrated during the I-B automatic configuration process, in which the small base station (SBS) performs its own installation and receives the basic configuration required for operation Fig. 9 [18]. As in [16], [20] and in [22] uses the backyard metropolis environment generation model for mm-Wave communications, which is expressed as follows:

$$pL(d)_{db} = pL(d_o)_{db} + 10nlog_{10}\left(\frac{d}{d_o}\right) + x\sigma \quad , \quad (6)$$

After a mm-Wave (Sc), equation (a) shows the direction is reinforced by the $pL(d)$ At scale d/(d o), functionality or the shadowing virtue reflects the point outdistance;

$$G_{db}(\varphi, \Theta) = \mathrm{G_m(dB)} - 14\left(\frac{\emptyset, \Theta}{\emptyset - 3dB}\right),^2 \quad (7)$$

$$G_m(dB) = \left(\frac{18\pi}{8.76\emptyset - 3dB\Theta - 3\mathrm{dB}}\right), \quad (8)$$

G_m represents the total beam gain of $\emptyset - 3dB\ and\ \Theta - 3\mathrm{dB}$, represents the beam width or power increased by half and represents $\emptyset$ the beam azimuth and Θ core inclination.;

$$P_r(d)_{db} = P_t(DBm) + G_{db}(\emptyset, \Theta) - PL(d)_{db} \quad (9)$$

Where equation (b) shows that P_t is the millimeter wave (mm-wave) single carrier (SC) Transmit (Tx) power [20].

$$\Re_t = \max\{d | P_{rmax}(d) \geq P_{th}\} \quad (10)$$

P_{th} is the power level, which depends on the sensitivity of the receiver. In this document, the required level of "MCS Zero" is selected. The horizontal coverage area's radius, $\Re_{cov}$, is a function of $\Re_t$.

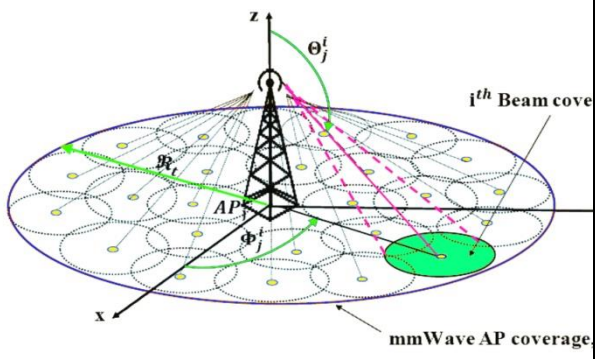

Fig.10. MM-Wave 3D beam setup.

The fixed beam configuration strategy is used because each mm-Wave deployed is equipped with a set of fixed beams to cover its coverage area. Fig. 10 uses 3D mm-wave beam setup as in order to cover the entire corner space between the AP and the UE, a large number of training frames must be sent. This standard solves the problem of link quality degradation caused by UE mobility by using beam optimization technology to find TX/RX beam pairs to maintain the link [16].

VII. System Model

The fast growth of wireless network services and use cases prompted the development of LTE, which aimed to improve mobile broadband connections using a flattened IP network. By 2030, mobile data traffic is estimated to have increased to 5 zettabytes per month. Consider a three-tier HetNet in which a UHF-based macro base station (MBS) is deployed in the center of a 500-meter circle, with low-power small base stations (SBS) covering the UHF and mmWave frequency bands uniformly layered on the MBS. With the goal of improving network KPIs, we focus on 5G networks and investigate the integration of model-free reinforcement learning with 5G technology. We use a variety of traffic scenarios to test key KPIs, such as throughput, latency, and packet drop rate. The 5G service categories uRLCC and eMBB are employed in particular, with uRLLC requiring high dependability and low latency and eMBB requiring high throughput. For mmWave frequencies, the dual-slope path loss model also appears to be overly complex. The uplink and downlink associations with the same base station are indicated by dashed arrows on the left and right, characterizing the behavior of the linked scenario. Decoupling is shown by single dashed arrows, which show uplink and downlink affiliation with different base stations. The behavior of the dual-slope path loss model is depicted in red circles for UHF macro base stations and UHF small base stations. We build a multi-agent Q-learning method for joint power and resource allocation to handle the coexistence problem of uRLLC and eMBB traffic over a 5G network, with the goal of balancing latency and reliability of uRLLC users. The suggested algorithm takes advantage of the time-frequency grid's flexibility, which was established in the 5G standard, to assign resources to users based on their requests. Every scheduling interval, our multi-agent Q-learning method is used to execute joint power and resource block allocation for each 5G NodeB (gNB). Because the transmission and queuing delays are the key impediments to meeting the 1 msec latency criterion, improving latency necessitates minimizing both. Furthermore, increasing dependability reduces the requirement for re-transmission and packet segmentation at the Radio Link Control (RLC) layer, which helps to reduce transmission time.

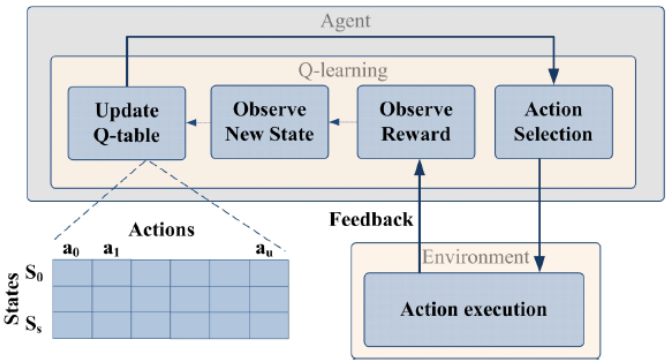

Fig.11. block diagram of Q-learning.

Fig. 11 shows the Q-learning method as furthermore, queuing delays are a direct result of scheduling delays. As a result, we provide a reward mechanism that has been carefully designed to solve uRLLC users' reliability, transmission, and queuing delays. In addition to Poisson traffic, we test the algorithm's performance in the presence of Constant Bit Rate (CBR) traffic. We show that our approach beats the baseline algorithm with a 4 percent reduction in Packet Drop Rate (PDR) and lower latency for large traffic loads. The following techniques are meant to attain the desired objectives based on this literature and having the statement of the problem:

- A mathematical model that can be used to calculate path loss for various path loss models.

- The breakpoint distance from the first Fresnel zone is calculated using a mathematical model.
- Calculate the path loss as a function of the break point distance using mathematical equations.
- Calculate the simulation's input parameters.
- Use the MATLAB and NYUSIM simulators to run simulations.
- Different route loss models were used to simulate path loss analyses for different frequency bands (38, 60, and 73 GHz) in the interior setting (free space, CI, and two rays).
- Path loss analysis simulation for several frequency bands with variable breakpoint distance.
- Break point distance simulation at various carrier frequencies, transmitter, and receiver heights.

VIII. System model and Mathematical Formulation

A system model for an interior setting with both LOS and NLOS conditions is displayed. The microcell's base station provides mmWave access link connection to all UEs and access points in an indoor environment. The communication system continues with greater signal quality when the environment is clear of barriers and the UE is within LOS of the BSs. Any impediment, such as a human barrier, ground reflection, or others, causes communication to be disrupted or lost. As Fig. 12 shows An indoor mmWave network scenario for 5G platforms, furthermore, these impediments cause increased route loss, which results in lower received power.

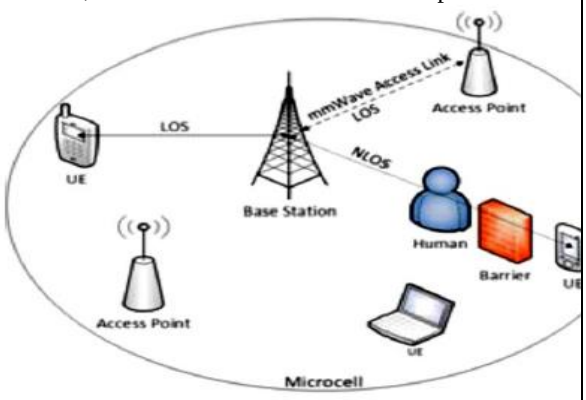

Fig.12. For 5G systems, an indoor mmWave network scenario.

IX. Path loss model

Path Loss Models will need to be constructed across a wide range of frequency bands and operating conditions to effectively examine the performance of 5G systems, particularly in an interior environment, where the received power is given as:

$$P_r(d) = P_t G_t A_r \frac{1}{4\pi d^2} \quad (11)$$

Where rP stands for reception power, tP stands for transmitter power, and tG stands for transmitter antenna. The effective area of a reception antenna is rA, and the distance between the transmitter and the receiver is D. The received power is inversely proportional to the separation distance between the user and the base station, according to the provided equation. The receiver antenna gain Gr has a relationship with the Effective area, which can be represented as:

$$G_r = \frac{4\pi}{\lambda^2} A_r \quad (12)$$

From equations (1) and (2), the following may be deduced:

$$P_r(d) = P_t G_t G_r \frac{\lambda^2}{(4\pi d)^2}$$
$$P_r[dBm] = P_t[dBm] + G_t[dB] + G_r[dB] - PL(d)[dB]$$

(13)

The received single power is r P, the sent signal power is t P, the transmitter antenna gain is t G, the receiver antenna gain is rG, and the average path loss at distance d is PL (d). If the antennas have the same gain (t G and r G are both one), the route loss equations are as follows:

$$PL = \frac{(4\pi d)^2}{\lambda^2} \quad (14)$$

The route loss is calculated using the logarithmic scale as follows:

$$PL(dB) = 20\log\left(\frac{4\pi d}{\lambda}\right) \quad (15)$$

Assume that c/f is equal to c/f, where f denotes frequency. The equation for millimeter wave now reads:

$$PL(dB) = 20\log\left(\frac{4\pi f \times 10^9}{c}\right)$$
$$PL(dB) = 20\log\left(\frac{4\pi d f \times 10^9}{3 \times 10^8}\right)$$

$$PL(dB) = 20\log\left(\frac{4\pi}{3}\right) + 20logf + 20logd$$
$$PL(dB) = 32.44 + 20logf + 20logd \qquad (16)$$

X. CI Path Model

One of the most prevalent route loss models is the CI free space reference distance path loss model. The CI model can be used to frequencies greater than or less than 6 GHz. This model is simple, accurate, and superior to others because it requires fewer parameters. The CI route loss is stated in the equation below.

$$PL^{CI}\ (f_c, d)[dB] = FSPL(f_c, d_o)[dB] + 10nlog_{10}(\frac{d}{1m}) + X_\delta^{CI}$$

(17)

Where d denotes the distance between TX and RX, n denotes the path loss exponent, and X δ denotes the shadow fading, which is a Gaussian random variable with a mean of zero and a standard deviation in dB, and FSPL denotes Friis' free space path loss with a 1m reference distance. For the GHz frequency band, the FSPL is now:

$$FSPL(f_c, d_o)[dB] = 20\log_{10}\left(\frac{4\pi f_c d_o \times 10^9}{c}\right) \qquad (18)$$

The speed of light is denoted by c. The equation (8) can then be simplified by using d_o =1m. d_o,1m value equation becomes:

$$FSPL(f_c, 1m)[dB] = 32.44 + 20\log_{10} f_c \qquad (19)$$

a result, equation (7) can be stated in the following way:

$$PL^{CI}(f_c, d)[dB] = 32.44 + 20\log_{10} f_c + 10nlog_{10}d + X_\delta^{CI}$$

(20)

XI. Exploiting Dual Slope Path Loss Model

$$Lmm(d) = \begin{Bmatrix} \rho + 10\alpha_l \log(d) + \delta_l\ for\ LoS \\ \rho + 10\alpha_n \log(d) + \delta_n\ for\ NLoS \end{Bmatrix} \qquad (21)$$

Fixed route loss is determined by ρ = 32.4 + 20log(fmm) in equation 11, where fmm is the millimetre wave carrier frequency and d is the radial distance between base station and user measured in metres. For LoS and NLoS mmWave links, the path loss exponent is indicated by l and n, respectively. The shadowing influence in the LoS and NLoS mmWave links is expressed by l and n, A user is supposed to be in Los and NLoS at the same time, as shown in equations 22 and 23 such as;

$$P_1(d) = e^{-\beta d} forLoS \qquad (22)$$

$$P_n(d) = 1 - P_l(d)\ for\ NLoS \qquad (23)$$

The blocking parameter is computed using building measurements for the region of interest (ROI), including density and average blockage size in the considered area, and d is the distance between base station and user in meters. As calculated in eq.14 as follows:

$$\beta = \frac{-\psi \ln(1-w)}{\pi A} \qquad (24)$$

In eq. 24, (ψ) is the average building perimeter (m) in the study (w) area, is the fraction of land covered by buildings, and A is the average building area in m2. These characteristics are calculated for a range of real-world situations using the Quantum Geographic Information System (QGIS) application. After finding the $P_l(d)$ and $P_n(d)$ using equations (22) and (23), we calculate the route loss for each millimetre wave tier based on these probabilities. The single slope route loss model $L_{uhf}(d) =$ in dB for the UHF band is as follows:

$$L_{uhf}(d) = 20\log(4\pi f_{uhf}) + 10\alpha lof(d) + \delta_{uhf} \qquad (25)$$

f_{uhf} is the carrier frequency for the UHF band in equation 3.5, and d is the distance between the base station and the user in metres. In σ^2 in UHF link, the route loss exponent is given as α and uhf represents shadowing effect. The dual-slope path loss model is the outcome of these limitations. The dual slope path loss model $L_{uhf}(d) =$ in dB is presented for the UHF band:

$$L_{uhf}(d) = \begin{Bmatrix} \rho + 10\alpha_1 \log(d) + \zeta_{uhf} & d \le r_{th} \\ \rho + 10\alpha_1 \log(r_{th}) + 10\,\alpha_2 \log\left(\frac{d}{r_{th}}\right) + \zeta_{uhf} & d > r_{th} \end{Bmatrix}$$

(26)

Fixed route loss is provided by ρ = 32.4 + 20log (f_{uhf}) in equation 16, where (f_{uhf}) is the carrier frequency for UHF band, d is the distance between base station and user measured in metres, and (r_{th}) is the threshold radius for UHF macro and UHF small base stations. The value of the path loss exponent fluctuates according to the tiers after the threshold radius (r_{th}). For moderate and difficult conditions, α_1 and α_2 are two route loss exponents for below and beyond threshold radius. The shadowing effect σ^2 is expressed by the ζ_{uhf} log normal random variable uhf, which has a mean of zero and a variance of two.

XII. Performance Analysis

Because to open access, users can now connect to the best base station in the downlink and uplink, resulting in greater uplink and downlink data speeds as well as increased coverage probability. Although the effect is primarily noticeable in uplink data rates. Because dual slope path loss model now better forecasts the results as it switches data traffic towards small base stations, the effect of decoupling is more noticeable depending on the environment type when dual slope model is deployed on UHF macro base station and UHF small base station. The signal to interference + noise ratio was computed as follows:

$$SINR_{,dl} = \frac{P_{rx,dl}}{I_{dl} + N_o} \quad (27)$$

$P_{rx,dl}$ is the maximum downlink received power from the associated base station at the user, I_{dl} is the interference at that user, and N_o is the noise power.where NF is the receiver's noise figure, which is 10dB, and BW is the system's bandwidth.

$$I_{dl,k} = \sum_{all\frac{BS}{m}} P_{rx}, dl \quad (28)$$

Because they share the same frequency band, UHF macro base stations and UHF small base stations interfere with each other, but mmWave small base stations only produce interference for mmWave small base stations. Because different frequency bands are used for downlink and uplink communication, there will be no interference. $I_{dl,k}$ is the downlink interference at a certain k_{th} user in the downlink who is associated with a specific mth base station, hence all other base station powers constitute interference for that user. We determine the downlink data rate for M number of users connected with a specific tier using eq. 29 as:

$$R_{,dl} = \frac{BW}{M} \log_2(1 + SINR_{,dl}) \quad (29)$$

The network's sum rate is then calculated for each of the four cases: decoupled with dual slope (DDS), decoupled with single slope (DSS), coupled with dual slope (CDS), and coupled with single (CSS) to see which strategy produces the best results. Another metric we use to assess the system's success is rate coverage probability as the number of small base stations grows. The probability of coverage at a certain threshold is computed as;

$$P_{cov_\tau} = R_{,dl} > \tau \quad (30)$$

The following eq. 31 can be used to calculate the system's energy efficiency:

$$EE = \frac{SumRate}{TotalPower} \quad (31)$$

Because we know that energy efficiency equals output divided by input, the sum rate is the output, and the total power from all base stations is the input. In the same way, the uplink SINR,ul is as follows:

$$SINR_{,ul} = \frac{P_{rx,ul}}{I_{ul} + N_o} \quad (32)$$

$$I_{ul,k} = \sum_{all\frac{UE}{k}} P_{rx,ul} \quad (33)$$

$P_{rx,ul}$ is the maximum uplink received power from a certain user at a specific connected base station, I_{ul} is the uplink interference caused by other users, and N_o is the system's noise power. In uplink interference $I_{ul,k}$, all users connected to a UHF Small base station or UHF MBS, except user k, cause interference. Similarly, all users connected to the mmWave spectrum have their uplink interference estimated. We determine the uplink data rate for N number of users connected to a specific tier in uplink using eq. 34 as:

$$R_{,ul} = \frac{BW}{N} log_2(1 + SINR_{,ul}) \quad (34)$$

The likelihood of coverage at a certain threshold is computed as follows:

$$\mathbb{P}_{cov_{(\tau)=R,ul>\tau}} \quad (35)$$

XIII. Coupled and Decoupled with Single Slope and Dual Slope Path Loss Model

The downlink and uplink of cellular networks have been coupled since the introduction of wireless communication, which means that mobile equipments have been constrained to connect with the same base station in both downlink and uplink directions. The downsides of this restriction are reinforced by new trends in network increasing density and cellular data consumption, hinting that it should be re-examined. When compared to competing technologies that give equal or lower advantages, decoupling can result in dramatic advances in system performance, reliability, and power efficiency at a reduced cost. According to the study, the network is structured such that users can connect to multiple base stations in the uplink and downlink, a process known as decoupling, in order to achieve larger gains in a dense hybrid heterogeneous environment. We will evaluate the performance of our suggested scheme, which is decoupled with dual slope (DDS), to three alternative schemes, which are decoupled with single slope (DSS), coupled with dual slope (CDS), and coupled with single slope (CSS), in terms of data rates, network coverage, and energy efficiency.

XIV. Simulation Setup

The modelling findings for the indoor environment at several mmWave bands and Sub 6 GHz are shown in this section. To improve the received power and throughput, different path loss models with respect to distances and breakpoint distances were investigated. At 38 and 73 GHz, the directional PDP was also investigated. MATLAB and NYUSIM software are used to model the results. With 2x2 and 64x16 antenna topologies and 10 RX random sites, we used NYUSIM to mimic directional PDP for both 38 GHz and 73 GHz. For Modeling of free space route loss in mmWave and sub-6 GHz bands

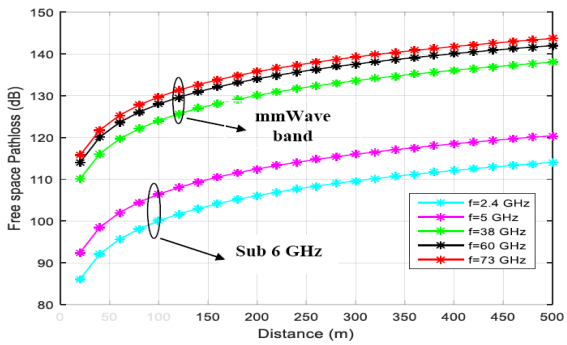

Fig.13. Distance vs. Free Path Loss.

Fig.13 depicts the link between TX-RX separation distance and free space path loss for various carrier frequencies.

Because of the small wave length of mmWave, which is easily occluded, route loss is substantially higher than at sub-6 GHz.

Table 5
Effect of increasing carrier frequency on route loss and received signal power.

Frequency (GHz)	Path loss (dB)	Received signal power (dBm)
2.4	76.3	-46.3
5	82.7	-52.7
38	100.3	-70.3
60	104.3	-74.3
73	106	-76

Table demonstrates the effect of increasing carrier frequency on route loss and received signal power for a separation distance of 65 m and a transmit power of 30 dBm. Now Two ray path loss models plotted at mmWave bands.

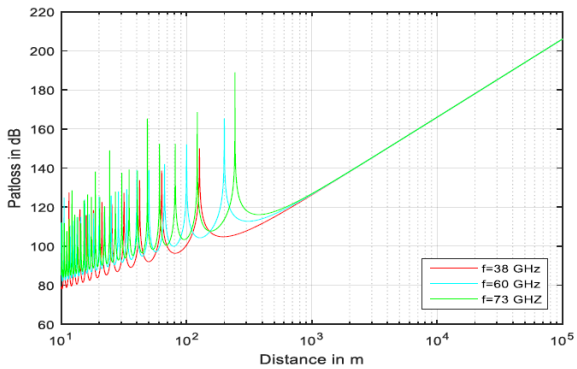

Fig.14. Loss of two ray paths vs. distance

A sinusoidal wave is formed by the route loss. These waves will continue until they reach a point where they will stop. Only the path loss at 73 GHz increases linearly with distance beyond that in Fig. 14. For mmWave bands and below 6 GHz, a CI path loss model is used.

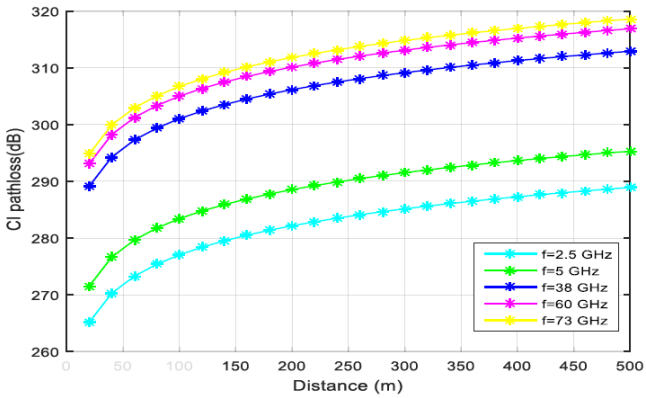

Fig.15. Distance vs. CI route loss.

Fig. 15 shows the link between CI path loss and distance at sub-6 GHz and mmWave frequencies. For mmWave bands, a comparison of the CI and the free space path loss model is made.

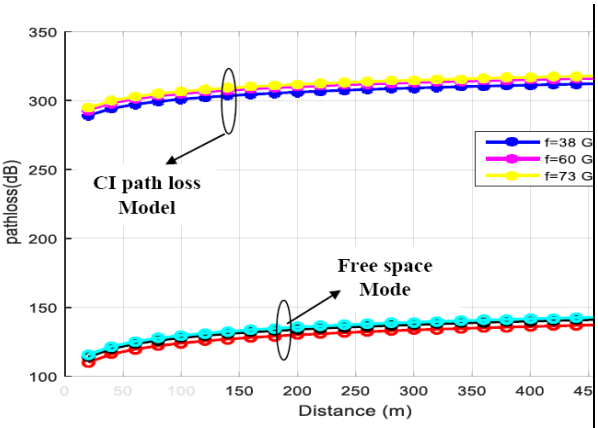

Fig. 16. For the CI and free space path loss models, path loss vs. distance is plotted.

Fig.16 depicts the relationship between free space path loss and break point distance for various transmitter heights with a receiver height of 0.5 m and a separation distance of 500 m. As the break point distance increases, the route loss increases with each height of transmitter. The point at which a direct signal is reflected is referred to as the "break point. As a result, we conclude that the received signal power is greater when the break point is near the transmitter than when the break point is at the cell boundary.

Table 6

Input parameter used in the above simulation.

Input parameters	Value
Carrier frequency	38/ 60/ 73 GHz
Transmit power	30 dBm
RF Bandwidth	800 MHz
Scenario	UMi
Environment	LOS/NLOS
Height of transmitter	1 m
Height of receiver	0.5 m
TX-RX separation	10-500 m
Number of RX locations	10
TX array Type, N_t	ULA,2,64
RX array Type, N_r	ULA,2,16
TX and RX antenna Spacing	0.5 λ
Azimuth and elevation HPBW for TX and RX	10^0

We demonstrate the performance of our suggested model in relation to various network parameters. We examine a circular cell with a radius of 500 metres, in which the SBS and UEs are uniformly spread across the entire geographic region and the MBS is fixed in the circle's centre. The transmission power of all user equipment is 20 dBm. For a certain number of tiny base stations and N=100, the likelihood of forming a downlink association varies (DDS-M) as:

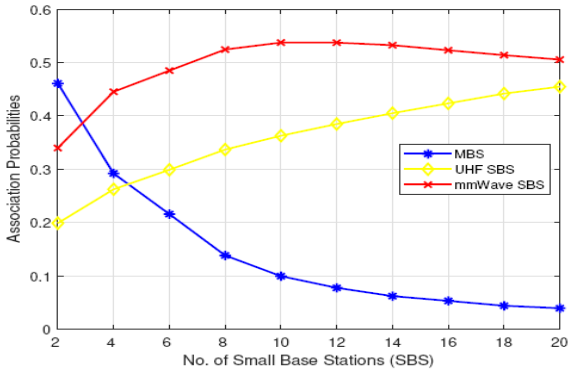

Fig. 17. certain number of tiny base stations and N=100, the likelihood of forming a downlink association varies (DDS-M.

Now for a certain number of tiny base stations and N=100, the likelihood of forming a downlink association varies (DDS-H).

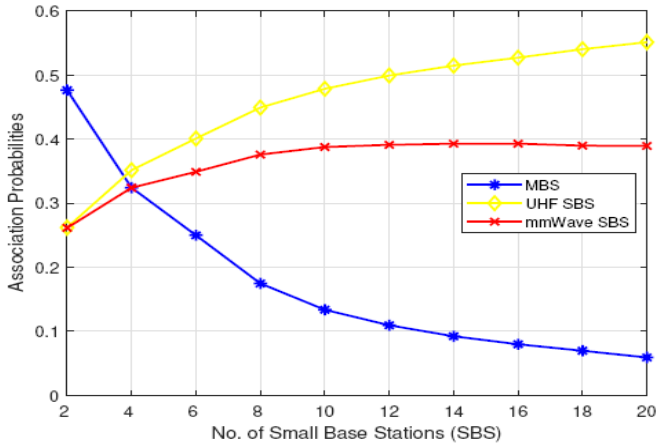

Fig.18.tiny base stations and N=100, the likelihood of forming a downlink association varies (DDS-H).

Because decoupling is affected by the environment, we assess our proposed scheme's performance in both moderate and hard environments. The association probabilities of our suggested scheme decoupling with dual slope (DDS) in mild and hard conditions are shown in Fig. 17 and Fig. 18 For The network's downlink total rate for different numbers of tiny base stations, N=100, in moderate and hostile settings (DDS).

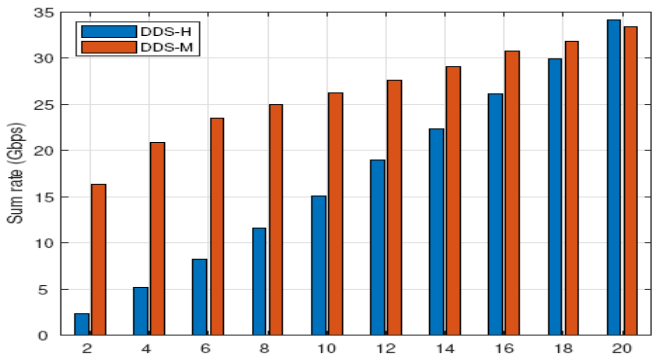

Fig.19. The network's downlink total rate for different numbers of tiny base stations.

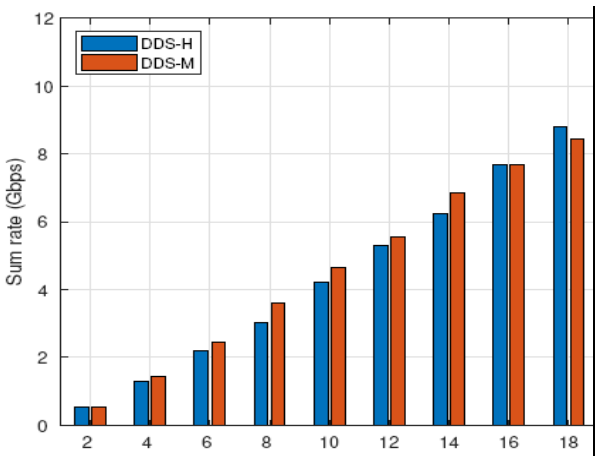

Fig. 20. The network's uplink total rate for different numbers of tiny base stations, N=100, in moderate and hostile settings (DDS).

Fig.19 and Fig.20 illustrate a comparison of the network's downlink and uplink sum rate in mild and hard settings, respectively, using the decoupled with dual slope (DDS) model. Because a larger number of users are linked to a mmWave small base station, a higher downlink sum rate can be attained in a moderate environment rather than a hard one.

Table 7
Parameters used in the above simulation

Symbol	Parameter	Value
f_{mm}	mmWave carrier frequency	73 GHZ
f_{uhf}	UHF carrier frequency	2.4 GHz
BW_{mm}	mmWave bandwidth	2 GHz
BW_{uhf}	UHF bandwidth	20 MHz
α_1 , α_2	Dual slope PLE for MBS (Moderate)	3,4
α_1 , α_2	Dual slope PLE for MBS (Harsh)	4,5
β_1 , β_2	Dual slope PLE for UHF SBS (Moderate)	2,4
β_1 , β_2	Dual slope PLE for UHF SBS (Harsh)	3,4
α_l , α_n	LoS/NLoS PLE for mmWave	2, 3.3
Bf	Biasing factor for mmWave	10 dB
R_{min}	Rate thershold	2Mbps
$P_{tx,1}$	MBS transmit power	46 dBm
$P_{tx,2}$	SBS transmit power	30 dBm
$P_{tx,3}$	UE transmit power	20 dBm
rad	radius of the circle	500 m
$r_{th,m}$	Threshold radius of MBS (Moderate)	350 m

The simulation requirements for these scenarios are based on the urban dual strip model proposed by the 3rd Generation Partnership Project (3GPP). Table 9 shows the comparison between different SC types and 5G macro cellular networks.

Table 8
For 5G cellular networks, a comparison of different types of small cells is made [1].

No.	Pico	Femto	Micro	Macro
Bandwidth(MHz)	20	30	30,40,50	60-85
Output Power (W)	0.30 -0.2	0.350	3-20	50-100
Users	5-18	35-100	300	2000+

Table 9
Simulation of mm-wave Mesh Network Parameters [48].

Noise of Density	696dBm/Hz	696dBm/Hz
No. of BSs	4	360
Path Loss	3GPP	[12]
Beam Pattern	3GPP	IEEE802.11ad
Tx Power	50dBm	20dBm
Antenna Height	30m	6m/30m (Sc-BS/Gw)
Antenna Gain	20dBi	36dBi
Carrier Frequency	4.0GHz	80GHz
Bandwidth	20MHz	2×2.16GHz
Parameter	LTE	mmWave SC-BS

A few 500 meters of macrocells (ISD) are presumably deployed in 3000 meters, and one macrocell is chosen as the evaluation cell in Table 10. WL One MC and a cluster of k number of indoor SCs/SBSs were used to create Computing Software (SBS) with self-optimization [1].

Table 10
The Proposed mm-Wave HetNet clusters simulation parameters [20].

Parameter	Value
Number of MCs	4
Number of SCs per MCs, N	10-60
Operating Frequency in (GHz) (Macro/ Femto / mm-wave)	3.1/ 3.5/4.0/4.5 60/80/100/150
Bandwidth (Macro/ Femto/ mm-wave)	100MHz/ 100MHz/ 4GHz
BS Height (Macro/ Femto/ mm-wave)	30m/20m/4m
eNB ISD	600m
Simulation Period, T	130s
Threshold Received Power, P_{th}	-80dBm

Table 10 lists the simulation's parameters and their corresponding values.

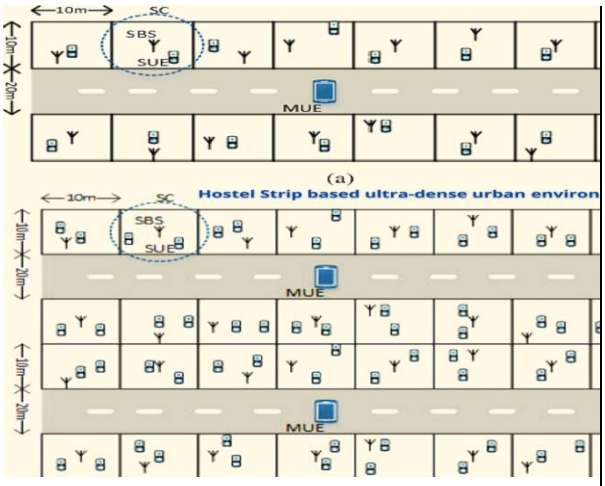

Fig.21. Ultra-dense urban simulation world based on the Hostel Strip [1].

Since Macro user equipment (MUEs) and clusters of Structured Cabling System (SCs) may take any place in the MC's coverage area, different interference scenarios arise. Three different MUE and SC cluster location scenarios were considered for the simulation model as shown in Fig. 21 [1]. For low-level interference, the two guard band simulations shown in Fig. 22 are also used in simulation scenario 1. In contrast, the Macro Consumer Equipment (MUE) is located near the mobile broadband system and not near the SC cluster. Mobile communications (MC) (MBS) However, due to the over density of structured cabling systems (SC), the coexistence interference is still very strong, as shown in Fig. 22 (Scenario 1) [1].

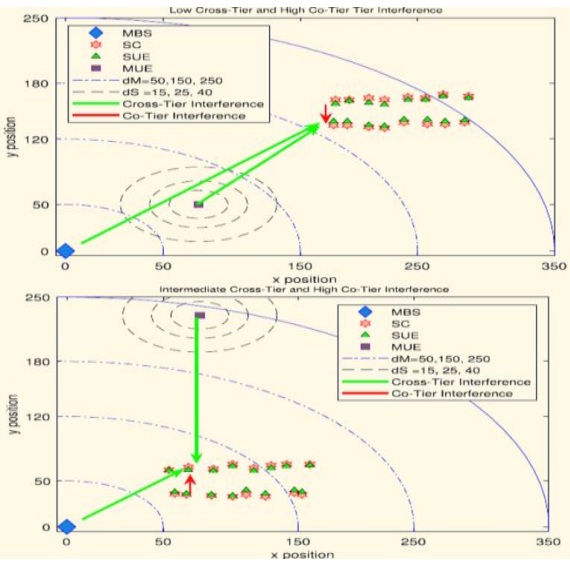

Fig.22. Scenario 1, Scenario 2 are simulated [1].

The simulation model of the two cover strips shown in Fig. 21 can also be used to simulate the interference between the layers in the second scheme. In this case, the Macro User Equipment (MUE) is isolated from the MBS and located in the center of the cell. This is the SC cluster. Since MBS and MUE are different from SC clusters, compared with scheme 2, the interference between layers in scheme 1 is smaller, as shown in Fig. 22 (Scenario 2) [1].

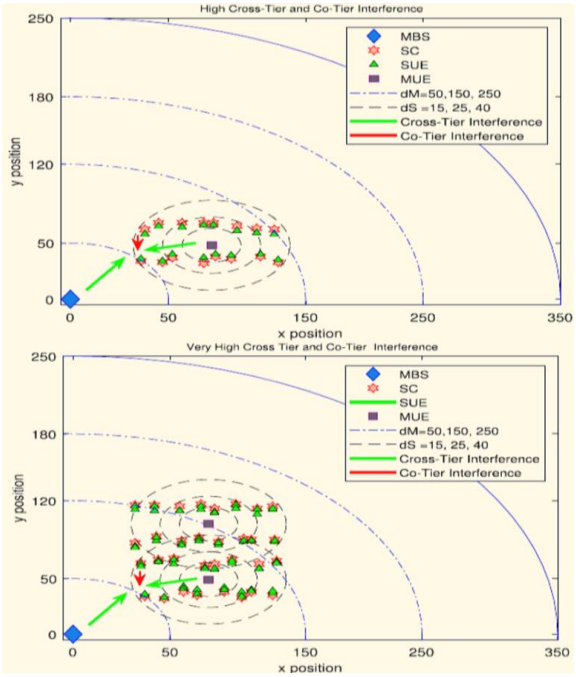

Fig.23. Scenario 3, Scenario 4 are simulated [1].

Wiring is very tight; there is much collaboration (SC). However, in this case, the MUE is connected to the mobile broadband system (MBS), which can cause strong interference between SCs near the macro market equipment (MUE). In this case, the MUE is located in the middle of the SC cluster, next to the MBS [1]. In simulation scenario 4, the four-lane protection simulator shown in Fig. 23 was used: extremely high interference. The simulated scene reflects the ultra-high density in the urban scene. Compared with Simulation Scheme 1-3, Simulation Scheme 1-3 uses Macro User Equipment (MUE) and User Equipment and System (SUES) more than twice. The two MUs are located in the center of the SC (Structured Cabling System) cluster, which in turn is located near the MBS (Mobile Broadband System) [1].

Table 11
Simulation Parameters.

Parameter	Value
Threshold received power, $Pmcs0$	-80dBm
Threshold received power, Pth	-77dBm

Simulation steps	130
UE speed, V	3 m/s
$\Phi{-}3dB$ /$\Theta{-}3dB$ of mm-Wave beam	Different
Num. of total beams mm-Wave AP	94
Height of mm-Wave AP/UD	4m/ 0.85m
TX Power of mm-Wave AP	12dBm
Num. of APs Mm-Wave	2
No. of MBS	2
No. of SCs	17,34
No. of MUEs	1,2
No. SUEs	1,2
Radius of MC	360m
Radius of SCs	15m
Learning Rate,α	0.6
Discount Factor Γ	0.10
Number of iterations	76000
Operating Frequency	3.0GHz

In particular, when a certain beam width is configured for mm-Wave AP, the number of beams in a fixed direction is fixed. Table 12 lists the main parameters of the simulation.

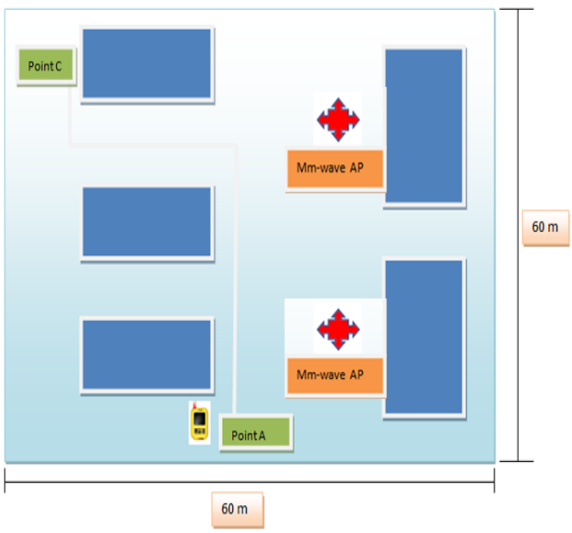

Fig.24. Two mm-Wave is deployed in the simulation area.

Fig. 24 shows that the UE traverses the location of the proposed device from point A to point C at a speed of 4m/s. As shown in Fig. 24, the mm-Wave access point in this simulation is used to provide mm-Wave services to provide different orientations UE with a beam on the target area.

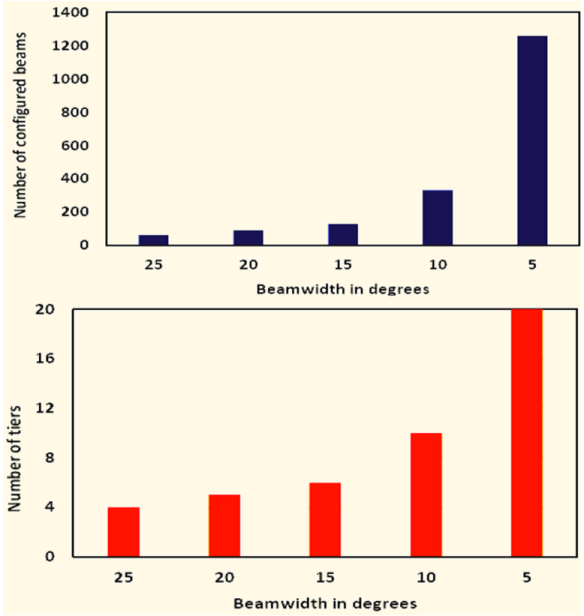

Fig.25. A number of optimized beams and beams' tiers for mm-Wave AP with different beam width values [16].

Fig. 25 shows that reducing the beam bandwidth and vice versa increases the total number of beams/interruptions required to cover the entire EU space of the millimeter-wave access point.

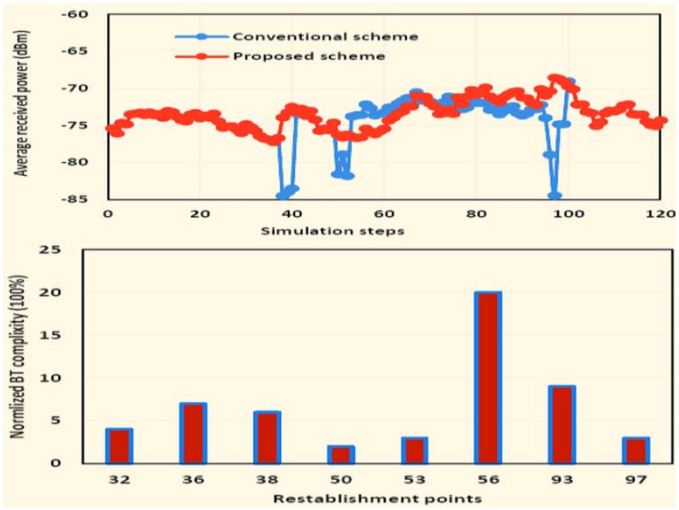

Fig.26. (a) Average power on the EU path and **(b)** BT complexity standardized [16].

Fig. 26(a) shows the average received power at 300 from point A to point C at the UE along the user path. Fig. 26(a) shows that the proposed scheme provides a higher average received power to the UE than the conventional path scheme. Fig. 26(b) shows

the normalized complexity at the restoration point along the route of the UE. Fig. 26(b) shows that the proposed system is comparable to the traditional complex search BT, and significantly reduces the complexity of BT.

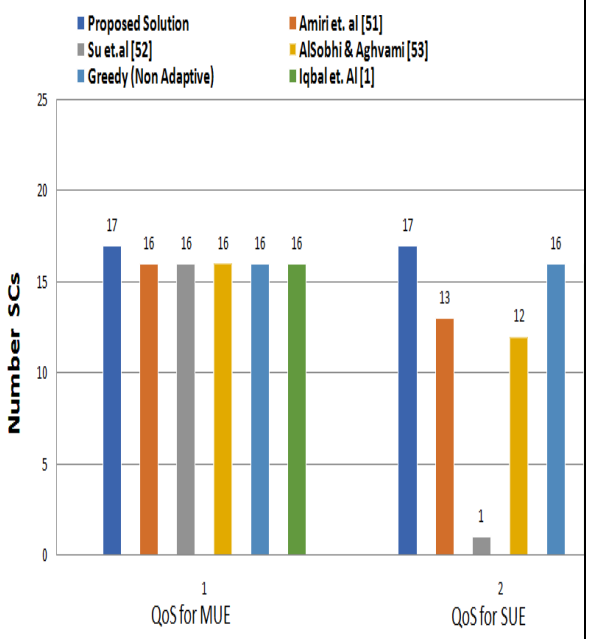

Fig.27. Scenario 1 of low cross tier interference is simulated.

The results from Fig. 27 low cross-tier interference scenario 1 are summarized as bar graphs in Fig. 27 to compare the proposed method's performance to other state-of-the-art methods and the greedy power allocation algorithm.

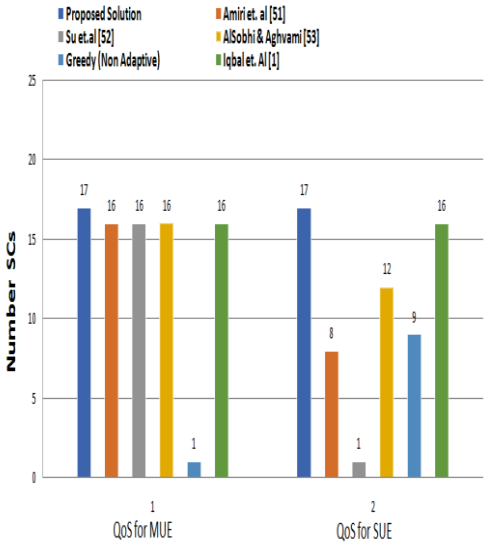

Fig.28. Intermediate cross tier interference Scenario 2 is simulated.

The results from Fig. 28 Intermediate cross-tier interference scenario 2 are summarized as bar graphs in Fig. 28 to compare the proposed method's performance to that of existing state-of-the-art methods and the greedy power allocation algorithm.

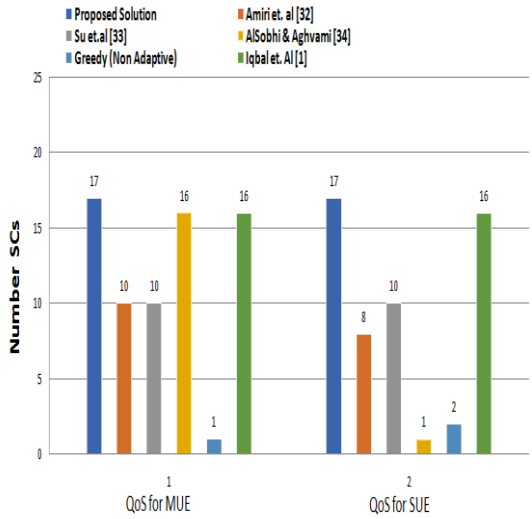

Fig.29. Scenario 3 of High cross tier interference is simulated.

The results from Fig. 29 High cross-tier interference scenario 3 are summarized as bar graphs in Fig. 29 to compare the proposed method's performance to other state-of-the-art methods and the greedy power allocation algorithm.

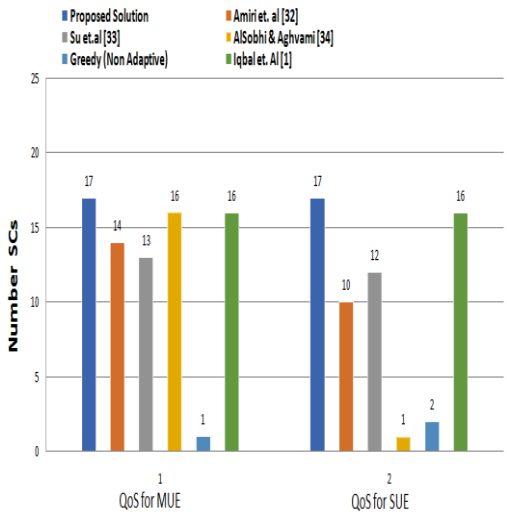

Fig.30. Scenario 4 of Very High cross tier interference is simulated.

The results from Fig. 30 extremely High cross-tier interference scenario 4 are summarized as bar graphs in Fig. 30 to compare the proposed method's performance to other state-of-the-art solutions and the greedy power allocation algorithm. In all three simulated scenarios, the proposed method outperformed state-of-the-art solutions and greedy power allocation algorithms, providing minimum QoS standards for both MUEs and SUEs, simultaneously up to 17 SCs. It is obvious that the proposed strategy not only effectively mitigates cross-tier and co-tier interferences, but also maintains the balance between MUEs and SUEs of different network tiers.

XV. Future Research of 6G Wireless Communications

The usage of a similar channel model structure and distinct parameter sets for different scenarios is advocated for standardized channel models used in 5G and older versions. Many channel models are limited to terrestrial and millimeter-wave frequencies. 6G radio communications must be carefully evaluated utilizing the overall structure of the conventional channel model as 6G radiation linkages become heterogeneous and have diverse wavelength ranges. The size of data grows rapidly when more frequency bands, locations, and antennas are added, and it becomes too large to be processed by traditional data processing methods. The report highlights major trends such as forecasts, systematic and in-depth analysis, and 6G technologies. As shown in Fig. 8, 6G wireless links operate in different frequency bands and scenarios. There are significant differences in acoustic channel signaling and the channel properties of each channel.

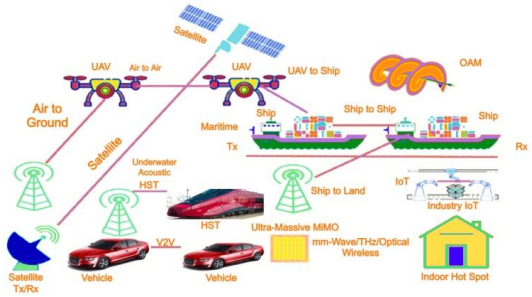

Fig.31. 6G broadband channels come in various forms.

Machine learning is an efficient and universal platform in the 6G wireless network. It has functions such as ubiquitous to humans and machines, secure and nearly instantaneous wireless connection, lane loss, and shadow attenuation. These features can provide a wide range of features at this time Broad channel performance. How does multipath fading lead to a fine-scale channel response. The ML model is a computer system or a trained model that learns the characteristics of the system (which cannot be described by a clear mathematical model). The measurement model and the ray-tracing model are two deterministic channel models: clustering, intelligent agent interaction and regression are tasks performed by machine learning models.

Table 12
Key technologies of 5G systems [2].

Technologies	Advantages	Disadvantages
Massive MIMO [2,10]	Noise reduction and fading. Support for a large range of devices. Help for a variety of quality of service (QoS) options. Massive traffic control.	Signal processing demands are high. Manufacturing costs are high. Complicated computations
Full Duplex [2,11]	Various applications. Massive traffic control. Collaboration and integration of many technologies.	Multiple radios are needed. Self-interference is a problem for you.
Energy harvest based [2,12]	Waste recycling is improved. Various applications.	Rely on a variety of energy sources. Energy transfer is extremely important.
Multi-tier communication [2,13]	SDNs provide assistance. Resolution of QoS problems for cell-edge users.	Upstream connection user exacerbation. Downlink asymmetrical power control.
Ultra-dense networks [2,14]	BS clustering and collaboration. Support for frequency reuse in multiband.	Restricting user association. A more effective power control technique is needed.
mm-Wave [2,15]	Applications that use SDNs are supported. Support for inter-BS collaboration. Help for increased bandwidth and energy	In inter-band with UHF, there is a compatibility problem. Help for multiple hops with throughput degradation.

harvesting.

The use of the millimeter-wave (mm-Wave) band is a significant step forward in the development of heterogeneous networks (HetNet) for fifth-generation (5G) remote mobile phone systems [11]. The main technological evolutions for 5G to 6G realization are mentioned in Table 4. To make such extra electrical energy efficient, 5G supports Multiple Input Multiple Output (MIMO). Both frequency channels that are certain of the imperative blessings of 5G have a spectral bandwidth of more than 40 GHz. Various channel modeling techniques have been proposed to accurately characterize the fundamental channel based on the specific properties of many large fading channel models and small fading channel models. The characteristics of various forms of 6G radio channels are different.

Table 13
A technology that allow 6G opportunities, applications, and challenges that have been encountered [11].

New enabling technologies	Opportunities and applications	Technological challenges
Quantum technology	Robot localization	Limitation in hardware
New frequency bands	Bid data analysis	miniaturization of THz elements and
Smart metal surfaces	Joint communication and radar	Heat problem due to hardware
High accuracy	AR/VR/MR	Short rage at THz
Dense Arrays	Lower power directional transmission	High hardware power consumption
AI and Machine learning,	e-Health	Dark spots and blockage
Low latency sub-ms,	Sending and Localization for future	devices
High Speed Tbps,	Sensor fusion	Increased interference from new

Because the satellite communication channel is mostly utilized for LOS transmission, the received signal is usually consistent due to the scintillation impact of weather and the troposphere [11]. The deterministic model and the stochastic model are detailed definitions of the large-scale air-to-ground model and the two tiny UAV channel models. Deterministic models are used in exploration and ray tracing (for example, two-ray models). Underwater acoustic corridors and waterways are used as deterministic modeling methods. Table 13 shows the different 6G versions and technological developments.

Table 14
6G technology advances and possible trends [11].

6G System	Various Trends
Convergence of Control, Communication & Computing	Trend 1
Autonomous System & Cyber Robots	Trend 2
New Smart City	Trend 3
High Speed Internet Access in the Air	Trend 4
Increased Bits, Increased Spectrum, Higher Efficiency	Trend 5
End of the Smartphone Span	Trend 6 (From Trend 1 to 6 are Artificial Intelligence Internet on Things and Machine Learning)
Global Emergency Communication Rescue	Trend 7
Energy Efficiency from Arial to Volumetric Spectral	Trend 8
Emergency of Smart Surfaces and Environments	Trend 9
Holographic Communication (Extended Reality-XR)	Trend 10
Massive Availability of Big Data to Small Data	Trend11
Digital Twin Technology in Human	Trend 12
Wireless Tactile Network	Trend 13
From Self Organizing Network to Self Sustainable Networks	Trend 14 (From Trend 7 to 14 are Communication Network Science and

Information Theory)

In addition, the recovered energy enables internet of things (IoT) devices to perform communication and computing tasks on the uplink of the same spectrum. In Table 14, 6G technology advances and possible trends are shown as this is a detailed inspection of the different types of 6G channels, divided into three categories: all spectrum, global coverage and equipment scenarios. In recent years, drones have been increasingly used for civilian and military purposes. 3D display, high maneuverability, space-time discontinuity, and shadow of aircraft structure are some of the design features of aircraft. Drone channel. Air-to-air and air-to-ground connections are divided into two categories: wireless has a strong interest in satellite communications and is seen as a reliable way to provide convenient and affordable services for global access. The size and characteristics of the 6G channel are summarized in Table 15.

Table 15
Measurements and features of 6G channels summarized [19].

Wireless Channel	Measured Frequency Bands	Measured Scenarios	Channel Characteristics
Industry IoT channel	Sub-6 GHz	Industry IoT environments	Path loss varies, random variations occur, NLOS propagation occurs, large numbers of scatters exist, and multi mobility exists.
OAM channel	mm-wave	LOS and NLOS (reflection)	Degradation in reflection scenarios, multiplexing gain, beam divergence and misalignment
Ultra-massive MIMO channel	Sub-6-GHz, mm-wave, and terahert z bands	Indoor and outdoor	Non-stationary in space, channel hardening, and spherical wave-front
HST/V2V channel	Sub-6-GHz and mm-wave bands	Highway, urban street, open area, university campus, and parking lot; open land, hilly terrain, viaducts, tunnels, cutting*, stations, and intra-wagon (HST); highway, urban street, open area, university campus, and parking lot (V2V)	Non-stationary, effect of train/vehicle, velocity and trajectory variations, large Doppler frequency shift and Doppler spread
Underwater acoustic channel	2–32 kHz	Underwater environments	Doppler effects, high transmission loss, multipath propagation, time-varying
Maritime channel	2.4 and 5.8 GHz	From the UAV to the ship, the ship to the ship, and the ship to the ground	Time non-stationary, long contact distances, environment conditions, sparse scattering, sea wave movement, ducting effect over the sea floor, time non-stationary
UAV channel	2, 2.4, and 5.8 GHz	The terms "urban," "suburban," "rural," and "open field" (air to air and	Airframe shadowing, 3D random trajectory (large elevation angle), high mobility,

		air to ground) are used.	spatial and temporal non-stationary
Satellite channel	Ku, K, Ka, and V bands	GEO, LEO, MEO, and HEO	Attenuation due to rain/cloud/fog/ snow, extremely high Doppler frequency change and Doppler spread, frequency dependency, large coverage range, and long contact gap
Optical wireless Channel	Mainly 380–780 nm	Indoor, outdoor, underground, Underwater	Background noise effects, complex scattering properties for various materials, nonlinear photoelectric characteristics at the Tx/Rx ends
mm-wave/terahertz channel	26/28-, 32-, 39/40-, 61-, and 75-GHz bands (mm-wave); around 300 GHz (terahertz)	Indoor and outdoor	Wide bandwidth, high directivity, high path loss, blockage effects, atmosphere absorption, and more diffuse scattering are all factors to consider.

In very large-scale MIMO, thousands of antennas are used to improve the spectrum, energy efficiency, accuracy, reliability, and independence of wireless communication systems. A series of nano-plasmonic elements can provide data in the frequency range of 1 to 10 THz (within a few square millimeters). OAM's ability to improve through cross-departmental performance has attracted attention in many fields (especially in the telecommunications field). For the energy of the liquid, the electrons rotate around the propagation axis defined by OAM. The traditional MIMO theory can provide OAM-based communication under certain conditions.

XVI. Future Research Challenges

Fast and effective measurement of 6G channels requires high-performance signal equipment. All VNA sirens, turnkey Rohde and Blacks sirens, Key sight/National Instruments and NYU wireless parks, and national standard survey alarm technology are examples of millimeter-wave channels. Alarm clocks VNA (Vector Network Analyzer) are all models of millimeter-wave displays. This research conducted a high-level analysis of backhaul networks (wireless/wired) and 5G and 6G systems, including the latest developments, research opportunities, and challenges. Consistent with the previous theme, new developments in 5G cellular networks include mm-Wave networks and huge technologies based on MIMO antennas. Furthermore, distributed network architecture for ultra-dense 5G cellular networks is recommended. Most terahertz signals are based on VNA channel signals and have additional up/down converters for different terahertz frequency bands. In addition, 5G cellular networks are also studying the density of small cells, which can be reached without affecting the output signal. As a result, 6G channel measurements have become increasingly complicated, but they are still vital and useful, particularly in high-frequency bands, high mobility, long-distance communications, and more challenging situations. They're mostly utilized to link smart items, people, and industries together.

XVII. Conclusion

To provide orders of magnitude more bandwidth than existing communication systems, mm-wave communications could be a candidate for 5G mobile networks. To reduce the broad X2 backhaul traffic load caused by standard HOs signaling between dense mm-Wave SCs deployed, this paper proposes clustered mm-Wave HetNet architecture. More research into other features of millimeter wave mobile communication should be undertaken in order to optimize the advantages of millimeter wave mobile communication for 5G. This article discusses the main issues of resource management and how they are directly or indirectly related to each other. Furthermore, various comparisons between methods and schemes are made for the purpose of evaluating the solutions. Users' standards for QoS are increasing, and efficient RRM schemes must account for these factors as well. Energy management is an important and critical aspect of resource

management, and this paper addresses existing strategies for managing energy in a variety of settings. The implementations of 5G RAN, as well as its various essential elements, such as RRM, are also discussed. If any more improvements are required in this area, these characteristics on other frequency bands should be investigated as well. There has been a proposal for a HetNet architecture that includes microwave and mm-Wave frequencies. We also used the channel model simulator to analyse the directional power delay profile with received signal power, path loss, and path loss exponent (PLE) for both LOS and NLOS at 38 GHz and 73 GHz mmWave bands using uniform linear array (ULA) 2X2 and 64x16 antenna configurations for both LOS and NLOS at 38 GHz and 73 GHz mmWave bands for both LOS and NLOS (NYUSIM). The simulation results show the performance of several path loss models in the mmWave and sub-6 GHz bands. Because it considers all shadowing and reflection effects between transmitter and receiver, the path loss in the close-in (CI) model at mmWave bands is higher than that of open space and two ray path loss models. We have also done a comparison with recent models such as; Amiri, Su, Alsobhi, Iqbal and greedy (non adaptive), the proposed method not only increased MUE and SUE minimum capacities and reduced BT complexity, but also established a new minimum QoS threshold. We also discussed the future research of 6G. When compared to utilising the dual slope route loss model alone in a hybrid heterogeneous network, our simulation findings show that decoupling is more visible when employing the dual slope path loss model, which enhances system performance in terms of coverage and data rate. Then we produced three case studies and four different scenarios that analysed and demonstrated some of the concerns. In general, this article examines several designs and analyses the research issues that must be addressed in order to meet the technological requirements of the future 5G network. It also looks at how mm-Wave communications can be used in 5G networks. We also talked about the problems, measurements, models, and framework trends for the 6G wireless channels.

References

M. U. Iqbal, E. A. Ansari, and S. Akhtar, “Interference Mitigation in HetNets to Improve the QoS Using Q-Learning,” IEEE Access, vol. 9, pp. 32405–32424, 2021, doi: 10.1109/access.2021.3060480.

[2] T. Akhtar, C. Tselios, and I. Politis, “Radio resource management: approaches and implementations from 4G to 5G and beyond,” Wireless Netw, vol. 27, no. 1, pp. 693–734, Nov. 2020, doi: 10.1007/s11276-020-02479-w.

[3] S. Malathy et al., “A review on energy management issues for future 5G and beyond network,” Wireless Netw, vol. 27, no. 4, pp. 2691–2718, Apr. 2021, doi: 10.1007/s11276-021-02616-z.

[4] R. K. Saha, “Spectrum Allocation and Reuse in 5G New Radio on Licensed and Unlicensed Millimeter-Wave Bands in Indoor Environments,” Mobile Information Systems, vol. 2021, pp. 1–21, Apr. 2021, doi: 10.1155/2021/5538820.

[5] H. Fourati, R. Maaloul, and L. Chaari, “A survey of 5G network systems: challenges and machine learning approaches,” Int. J. Mach. Learn. & Cyber., vol. 12, no. 2, pp. 385–431, Aug. 2020, doi: 10.1007/s13042-020-01178-4.

[6] B. Li, Y. Dai, Z. Dong, E. Panayirci, H. Jiang, and H. Jiang, “Energy-Efficient Resources Allocation with Millimeter-Wave Massive MIMO in Ultra Dense HetNets by SWIPT and CoMP,” IEEE Trans. Wireless Commun., pp. 1–1, 2021, doi: 10.1109/twc.2021.3058776.

[7] Y. Xu, G. Gui, H. Gacanin, and F. Adachi, “A Survey on Resource Allocation for 5G Heterogeneous Networks: Current Research, Future Trends, and Challenges,” IEEE Commun. Surv. Tutorials, vol. 23, no. 2, pp. 668–695, 2021, doi: 10.1109/comst.2021.3059896.

[8] A. Yoneyama, F. Kemmochi, and H. Otsuka, “Pico-eNB Tx Power Optimization for Multiband HetNets with MCS Incorporating 1024-QAM,” presented at the 2021 International Conference on Information Networking (ICOIN), Jan. 2021. doi: 10.1109/icoin50884.2021.9333900.

[9] P. P. Ray, “A perspective on 6G: Requirement, technology, enablers, challenges and future road map,” Journal of Systems Architecture, vol. 118, p. 102180, Sep. 2021, doi: 10.1016/j.sysarc.2021.102180.

[10] M. Abbasi, A. Shahraki, Md. Jalil Piran, and A. Taherkordi, “Deep Reinforcement Learning for QoS provisioning at the MAC layer: A Survey,” Engineering Applications of Artificial Intelligence, vol. 102, p. 104234, Jun. 2021, doi: 10.1016/j.engappai.2021.104234.

[11] T. Sharma, A. Chehri, and P. Fortier, "Review of optical and wireless backhaul networks and emerging trends of next generation 5G and 6G technologies," Trans Emerging Tel Tech, vol. 32, no. 3, Oct. 2020, doi: 10.1002/ett.4155.

[12] J. Shuja, K. Bilal, W. Alasmary, H. Sinky, and E. Alanazi, "Applying machine learning techniques for caching in next-generation edge networks: A comprehensive survey," Journal of Network and Computer Applications, vol. 181, p. 103005, May 2021, doi: 10.1016/j.jnca.2021.103005.

[13] M. S. J. Solaija, H. Salman, A. B. Kihero, M. I. Saglam, and H. Arslan, "Generalized Coordinated Multipoint Framework for 5G and Beyond," IEEE Access, vol. 9, pp. 72499–72515, 2021, doi: 10.1109/access.2021.3079190.

[14] S. Albadran, "Evaluation of Development Level and Technical Contribution of Recent Technologies Adopted to Meet the Challenges of 5G Wireless Cellular Networks," Symmetry, vol. 13, no. 4, p. 635, Apr. 2021, doi: 10.3390/sym13040635.

[15] H. Mathur and T. Deepa, "A Survey on Advanced Multiple Access Techniques for 5G and Beyond Wireless Communications," Wireless Pers Commun, vol. 118, no. 2, pp. 1775–1792, Jan. 2021, doi: 10.1007/s11277-021-08115-w.

[16] K. Abdelgaber, A. Mubarak, and M. Salah, "EFFICIENT mmWAVE BEAM TRACKING FOR 5G AND BEYOND WIRELESS SYSTEMS," Sohag Engineering Journal, vol. 1, no. 1, pp. 25–33, Mar. 2021, doi: 10.21608/sej.2021.155712.

[17] X. Wang and M. C. Gursoy, "Coverage in Networks with Hybrid Terahertz, Millimeter Wave, and Microwave Transmissions," presented at the 2021 IEEE 18th Annual Consumer Communications & Networking Conference (CCNC), Jan. 2021. doi: 10.1109/ccnc49032.2021.9369465.

[18] A. H. Nalband, M. Sarvagya, and M. R. Ahmed, "Spectral Efficient Beamforming for mmWave MISO Systems using Deep Learning Techniques," Arab J Sci Eng, Apr. 2021, doi: 10.1007/s13369-021-05552-4.

[19] C.-X. Wang, J. Huang, H. Wang, X. Gao, X. You, and Y. Hao, "6G Wireless Channel Measurements and Models: Trends and Challenges," IEEE Veh. Technol. Mag., vol. 15, no. 4, pp. 22–32, Dec. 2020, doi: 10.1109/mvt.2020.3018436.

[20] A. S. Mubarak, H. Esmaiel, and E. M. Mohamed, "LTE/Wi-Fi/mmWave RAN-Level Interworking Using 2C/U Plane Splitting for Future 5G Networks," IEEE Access, vol. 6, pp. 53473–53488, 2018, doi: 10.1109/access.2018.2871059.

[21] R. M. Borges et al., "Integrating Optical and Wireless Techniques towards Novel Fronthaul and Access Architectures in a 5G NR Framework," Applied Sciences, vol. 11, no. 11, p. 5048, May 2021, doi: 10.3390/app11115048.

[22] L. Zhu, L. Yang, Q. Zhang, T. Zhou, and J. Hua, "Cluster-based energy-efficient joint user association and resource allocation for B5G ultra-dense network," Physical Communication, vol. 46, p. 101311, Jun. 2021, doi: 10.1016/j.phycom.2021.101311.

[23] S. Hashima, B. M. ElHalawany, K. Hatano, K. Wu, and E. M. Mohamed, "Leveraging Machine-Learning for D2D Communications in 5G/Beyond 5G Networks," Electronics, vol. 10, no. 2, p. 169, Jan. 2021, doi: 10.3390/electronics10020169.

[24] P. Pratim Ray, N. Kumar, and M. Guizani, "A Vision on 6G-Enabled NIB: Requirements, Technologies, Deployments and Prospects," IEEE Wireless Commun., pp. 1–8, 2021, doi: 10.1109/mwc.001.2000384.

[25] M. Servetnyk, W.-H. Hsiao, and A. Mukashev, "Performance Evaluation of Polarization Effects on 5G Clustered Delay Line Channels," presented at the 2021 23rd International Conference on Advanced Communication Technology (ICACT), Feb. 2021. doi: 10.23919/icact51234.2021.9370660.

[26] Y. Shi, M. Q. Hamdan, E. Alsusa, K. A. Hamdi, and M. W. Baidas, "A Decoupled Access Scheme with Reinforcement Learning Power Control for Cellular-Enabled UAVs," IEEE Internet Things J., pp. 1–1, 2021, doi: 10.1109/jiot.2021.3078188.

[27] L. Chen, B. Hu, S. Chen, J. Xu, and G. Xu, "QoE-Aware Resource Allocation for

Non-Orthogonal Multiple Access Enhanced HetNets," IEEE Trans. Cogn. Commun. Netw., pp. 1–1, 2021, doi: 10.1109/tccn.2021.3074944.

[28] X. Li, H.-N. Dai, M. K. Shukla, D. Li, H. Xu, and M. Imran, "Friendly-jamming schemes to secure ultra-reliable and low-latency communications in 5G and beyond communications," Computer Standards & Interfaces, vol. 78, p. 103540, Oct. 2021, doi: 10.1016/j.csi.2021.103540.

[29] B. P. S. Sahoo, S. Swain, H.-Y. Wei, and M. Sarkar, "Medium Access Strategies for Integrated Access and Backhaul at mmWaves Unlicensed Spectrum," presented at the 2021 Wireless Telecommunications Symposium (WTS), Apr. 2021. doi: 10.1109/wts51064.2021.9433686.

[30] A. Jain, E. Lopez-Aguilera, and I. Demirkol, "User association and resource allocation in 5G (AURA-5G): A joint optimization framework," Computer Networks, vol. 192, p. 108063, Jun. 2021, doi: 10.1016/j.comnet.2021.108063.

[31] L. Chen, B. Hu, G. Xu, and S. Chen, "Energy-Efficient Power Allocation and Splitting for MmWave Beamspace MIMO-NOMA with SWIPT," IEEE Sensors J., pp. 1–1, 2021, doi: 10.1109/jsen.2021.3076517.

[32] H. Ahmadinejad and A. Falahati, "Spectral efficiency in non-terrestrial heterogeneous networks with spectrum underlay access," Physical Communication, vol. 46, p. 101313, Jun. 2021, doi: 10.1016/j.phycom.2021.101313.

[33] P. Zhou, X. Fang, and X. Wang, "Joint Radio Resource Allocation for Decoupled Control and Data Planes in Densely Deployed Coordinated WLANs," IEEE Trans. Wireless Commun., pp. 1–1, 2021, doi: 10.1109/twc.2021.3053354.

[34] J. Kim, P. V. Astillo, V. Sharma, N. Guizani, and I. You, "MoTH: Mobile Terminal Handover Security Protocol for HUB Switching based on 5G and Beyond (5GB) P2MP Backhaul Environment," IEEE Internet Things J., pp. 1–1, 2021, doi: 10.1109/jiot.2021.3082277.

[35] S. Habibi, V. Solouk, and H. Kalbkhani, "Adaptive energy-efficient small cell sleeping and zooming in heterogeneous cellular networks," Telecommun Syst, vol. 77, no. 1, pp. 23–45, Jan. 2021, doi: 10.1007/s11235-020-00740-3.

[36] G. Eappen and T. Shankar, "Multi-Objective Modified Grey Wolf Optimization Algorithm for Efficient Spectrum Sensing in the Cognitive Radio Network," Arab J Sci Eng, vol. 46, no. 4, pp. 3115–3145, Nov. 2020, doi: 10.1007/s13369-020-05084-3.

[37] M. K. Shehzad, A. Ahmad, S. A. Hassan, and H. Jung, "Backhaul-Aware Intelligent Positioning of UAVs and Association of Terrestrial Base Stations for Fronthaul Connectivity," IEEE Trans. Netw. Sci. Eng., pp. 1–1, 2021, doi: 10.1109/tnse.2021.3077314.

[38] M. Wang, Y. Lin, Q. Tian, and G. Si, "Transfer Learning Promotes 6G Wireless Communications: Recent Advances and Future Challenges," IEEE Trans. Rel., vol. 70, no. 2, pp. 790–807, Jun. 2021, doi: 10.1109/tr.2021.3062045.

[39] S.-W. Ko, H. Chae, K. Han, S. Lee, D.-W. Seo, and K. Huang, "V2X-Based Vehicular Positioning: Opportunities, Challenges, and Future Directions," IEEE Wireless Commun., vol. 28, no. 2, pp. 144–151, Apr. 2021, doi: 10.1109/mwc.001.2000259.

[40] Y. Djeldjeli and M. Zoubir, "CP-SDN: A New Approach for the Control Operation of 5G Mobile Networks to Improve QoS," Eng. Technol. Appl. Sci. Res., vol. 11, no. 2, pp. 6857–6863, Apr. 2021, doi: 10.48084/etasr.4016.

[41] M. Al-Jarrah, E. Alsusa, A. Al-Dweik, and M.-S. Alouini, "Performance Analysis of Wireless Mesh Backhauling Using Intelligent Reflecting Surfaces," IEEE Trans. Wireless Commun., pp. 1–1, 2021, doi: 10.1109/twc.2021.3052370.

[42] F. Zhou, L. Feng, P. Yu, W. Li, X. Que, and L. Meng, "DRL-based Low-Latency Content Delivery for 6G Massive Vehicular IoT," IEEE Internet Things J., pp. 1–1, 2021, doi: 10.1109/jiot.2021.3064874.

[43] M. B. Rahaim, T. D. C. Little, and M. Hella, "Multi-Tier Heterogeneous Beam Management for Future Indoor FSO Networks,"

Applied Sciences, vol. 11, no. 8, p. 3627, Apr. 2021, doi: 10.3390/app11083627.

[44] M. Arif, S. Wyne, K. Navaie, S. J. Nawaz, and S. H. Alvi, "Decoupled Downlink and Uplink Access for Aerial Terrestrial Heterogeneous Cellular Networks," IEEE Access, vol. 8, pp. 111172–111185, 2020, doi: 10.1109/access.2020.3002328.

[45] S. Driouech, E. Sabir, M. Ghogho, and E.-M. Amhoud, "D2D Mobile Relaying Meets NOMA—Part II: A Reinforcement Learning Perspective," Sensors, vol. 21, no. 5, p. 1755, Mar. 2021, doi: 10.3390/s21051755.

[46] X. Jian, L. Wu, K. Yu, M. Aloqaily, and J. Ben-Othman, "Energy-efficient user association with load-balancing for cooperative IIoT network within B5G era," Journal of Network and Computer Applications, vol. 189, p. 103110, Sep. 2021, doi: 10.1016/j.jnca.2021.103110.

[47] K. Sakaguchi, G. K. Tran, and H. Ogawa, "MmWave meshed network with traffic and energy management mechanism," presented at the 2017 IEEE 18th International Workshop on Signal Processing Advances in Wireless Communications (SPAWC), Jul. 2017. doi: 10.1109/spawc.2017.8227745.

[48] K. SAKAGUCHI et al., "Millimeter-Wave Evolution for 5G Cellular Networks," IEICE Trans. Commun., vol. E98.B, no. 3, pp. 388–402, 2015, doi: 10.1587/transcom.e98.b.388.

[49] M. H. Khadr, H. Elgala, M. Rahaim, A. Khreishah, M. Ayyash, and T. Little, "Machine learning-based security-aware spatial modulation for heterogeneous radio-optical networks," Proc. R. Soc. A., vol. 477, no. 2248, Apr. 2021, doi: 10.1098/rspa.2020.0889.

[50] A. Saeed, O. Gurbuz, A. O. Bicen, and M. A. Akkas, "Variable-Bandwidth Model and Capacity Analysis for Aerial Communications in the Terahertz Band," IEEE J. Select. Areas Commun., vol. 39, no. 6, pp. 1768–1784, Jun. 2021, doi: 10.1109/jsac.2021.3071831.

[51] G. Caso, L. De Nardis, and L. Gavrilovska, Eds., Cognitive Radio-Oriented Wireless Networks. Springer International Publishing, 2021. doi: 10.1007/978-3-030-73423-7.

[52] Y. Ouyang, Z. Zeng, X. Li, T. Wang, and X. Liu, "A verifiable trust evaluation mechanism for ultra-reliable applications in 5G and beyond networks," Computer Standards & Interfaces, vol. 77, p. 103519, Aug. 2021, doi: 10.1016/j.csi.2021.103519.

[53] S. H. Alsamhi et al., "Green internet of things using UAVs in B5G networks: A review of applications and strategies," Ad Hoc Networks, vol. 117, p. 102505, Jun. 2021, doi: 10.1016/j.adhoc.2021.102505.